J. Fluid Mech. (1994), *vol.* 258, *pp.* 255–285

Multiple linear instability of layered stratified shear flow

By COLM-CILLE P. CAULFIELD†

Department of Applied Mathematics and Theoretical Physics, Silver Street, Cambridge, CB3 9EW, UK

(Received 22 January 1993 and in revised form 23 June 1993)

We develop a simple model for the behaviour of an inviscid stratified shear flow with a thin mixed layer of intermediate fluid. We find that the flow is simultaneously unstable to oscillatory disturbances that are a generalization of those discussed by Holmboe (1962), purely unstable modes analogous to those considered by Taylor (1931), and a new type of oscillatory disturbance at large wavelength. The relative significance of these different types of instability depends on the ratio R of the depth of the intermediate layer to the depth of the shear layer. For small values of R, the new type of oscillatory wave has both the largest growthrate for given bulk Richardson number Ri_0, and is also primarily unstable to disturbances propagating at an angle to the mean flow, i.e. such modes violate the conditions of Squire's theorem (1933), and thus the assumption of initial two dimensionality of such flows is invalid. For intermediate values of R, the Holmboe-type modes and the Taylor-types modes may have wavelengths and phase speeds conducive to the formation of a resonant triad over a wide range of Ri_0. Thus the presence of an intermediate layer in a stratified shear flow markedly changes its stability properties.

1. Introduction

In many geophysical flows, density differences in a fluid play a very significant role. Both the atmosphere and ocean are stratified (see Gill 1982). This ambient stratification often modifies markedly the behaviour of a flow from that of a flow with the same initial velocity distribution in a homogeneous fluid. Taylor (1931) was among the first to realize that the stability of a stratified fluid undergoing shear is very different from that of a homogeneous fluid. Indeed, counter-intuitively, flows that are stable in the absence of stratification may be destabilized by (statically stable) variations in the density field of the background flow. Such instability often leads to a breakdown of the flow, and mixing of fluid of different density, thus altering the background density field. It is known (see Turner 1973) that such mixing events, once the turbulence within them decays, can lead to a layering of the background density field, with regions of weak density gradient alternating with regions of strong density gradient. The stability of such layered fluids when the background flow once again becomes sheared is an important problem, which is not well understood. This paper is concerned with the analysis of a simple model for one mixed layer (i.e. a flow with two regions of strong density gradient) embedded within a region of shear, which still exhibits a rich variety of possible routes to instability and flow breakdown that are not present when the density gradient is either constant, or has only one region of strong gradient.

† Present address: Department of Physics, 60 St George St, University of Toronto, Toronto, Ontario, Canada, M5S 1A7.

After mixing events associated with flow instability in a sheared stratified fluid, the region of mixed fluid has been found experimentally not, in general, to match exactly the region of velocity variation, though typically this intermediate layer is wholly embedded within the shear layer (see Redondo 1989; Thorpe 1973; Linden 1979). Indeed extremely thin intermediate layers have been observed experimentally when the stratification is relatively strong (see Narimousa & Fernando 1987; Stephenson & Fernando 1991). As we shall see, flows with narrow intermediate layers have the potential for primary three-dimensional instability.

To investigate the significance of variation in the depth of a mixed layer relative to shear layer depth, we consider a three-layer density distribution, where the depth of the intermediate density layer is of arbitrary (smaller) depth relative to that of the piecewise linear shear layer. Since the velocity is taken to be piecewise linear, the background vorticity field is piecewise constant.

In §2, we review and re-interpret previous work by Taylor (1931) and Holmboe (1962) on two special cases of such flows. Taylor considered a three-layer flow where the intermediate layer extended over the full depth of the shear layer. He found that this flow is unstable to disturbances (which we shall refer to as T modes) moving with the mean speed of the shear flow for all values of the bulk Richardson number, Ri_0.

Holmboe considered a two-layer flow, which, provided Ri_0 is sufficiently large, is unstable to two disturbances, one moving upstream and the other downstream relative to the mean speed of the shear layer. We will refer to these unstable modes as H modes. At finite amplitude these modes equilibrate into disturbances, known as Holmboe waves which have been observed experimentally (Browand & Winant 1973). Holmboe waves are characterized by regions of overturning centred around the critical levels of the flow, where the phase speed of the linear instability equals the background flow speed. Numerical calculations of smooth profiles of velocity and density also predict the existence of such modes, provided that the characteristic lengthscale of the (single) region of gradient in density is significantly smaller than the characteristic lengthscale of the region of velocity gradient (see Hazel 1972, and, at finite amplitude, Smyth, Klaasen & Peltier 1988). Of particular interest is that these modes require the presence of stratification to grow, since for small values of Ri_0, the flow is unstable to a Kelvin–Helmholtz type instability, with phase speed equal to the mean speed of the shear layer. Using the concepts of Cairns (1979), we can identify all these modes with interactions of waves on the various interfaces of either vorticity or density.

Whereas, for the two cases considered before, at intermediate Ri_0 there is only one possible type of instability, we show that three-layer flows in general exhibit H and T mode instability at arbitrary Ri_0, and another type of instability appears, which in certain situations may be very significant to the mixing of the flow.

In §3, we derive the eigenvalue equation for a symmetric three-layer flow with arbitrary intermediate layer depth. We find that for this situation, the eigenvalue equation is bicubic in c.

In §4, we discuss the effect of a region of intermediate density on the growing modes predicted by the eigenvalue equation in terms of the possible interactions of interfacial waves. An important parameter is found to be the ratio, R, of the depth of the intermediate density layer to the shear layer.

For moderate values of R, at a given Ri_0, there are not only H modes, but also three-layer analogues of T modes. These T modes arise through a resonance between internal waves on opposite density interfaces, and have zero real phase speed in the frame of reference moving with the mean speed of the shear layer. There is also a previously undocumented region of instability. This region of instability consists of a pair of

oscillatory instabilities, with absolute phase speed (relative to the mean speed of the shear layer) appreciably less than that of the H mode, and thus likely to have regions of overturning at finite amplitude closer to the density interfaces. This mode implicitly requires the existence of a three-layer density distribution, and so we refer to it as the R mode.

We map the appearance and eventual dominance of T modes, and the disappearance of Holmboe-type modes for large R. This is to be expected, since at $R = 1$, Taylor found no Holmboe-type modes. We also discuss the behaviour of the roots of the eigenvalue equation for small Ri_0 where we find an approach to the existence of a region of Kelvin–Helmholtz type instability as $R \to 0$, related to the region discussed by Holmboe when $R = 0$. We note that the maximal growthrate for a given Ri_0 of an H mode increases as R is increased from 0 to a (global) maximum at $R \sim 0.1$. This is of significance because it is just such a mode which we expect to see in the laboratory.

Since both the R and H modes exist only in the presence of stratification, the very applicability of the initial consideration of two-dimensional disturbances as being the most unstable for a given two-dimensional flow is called into question. We discuss a theorem due to Yih (1955), which is essentially a generalization of Squire's theorem (1933) (who considered flow in a channel). A mode whose wavenumber vector is oriented at an angle to the mean flow can be identified with an equivalent mode with wavenumber vector parallel to a mean flow with a higher Richardson number. Thus if the maximal (at a given Ri_0) growthrate of a mode increases at a sufficient (well-defined) rate with Ri_0, Yih's theorem predicts that the mode travelling at an angle will, within linear theory, have a larger growthrate than all modes travelling parallel to a given flow. In this case, the flow is predicted to be primarily unstable to three-dimensional disturbances.

Although they are destabilized by the stratification, and do not appear in a homogeneous flow, two-layer H modes are always expected to be primarily unstable to two-dimensional disturbances. (The derivation of this result by Smyth *et al.* (1988) maximizes the growthrate with respect to wavenumber rather than with respect to Richardson number, though the conclusion is correct.)

Numerical calculations (Smyth & Peltier 1990) have established that in certain regions of parameter space there exists a region of primary three-dimensional instability for $Re \leqslant 400$ (defined using half the shear layer depth, and half the change in velocity across the shear layer) which may explain the three-dimensionality of the waves observed in the laboratory by Browand & Winant (1973) and Lawrence, Browand & Redekopp (1991).

As we show in §4, H modes for arbitrary R are still susceptible primarily to two-dimensional disturbances. However, at least initially, the growthrate for the R modes is such that they are expected to be primarily three-dimensionally unstable. For certain values of Ri_0, and α, and for small, but finite R (i.e. $R \leqslant 0.095$) these modes have larger growthrates than both the H and T modes at given Ri_0, and so there is a region of parameter space, where, by a correct application of Yih's (1955) theorem, the flow is subject to a primary three-dimensional instability in this inviscid limit. These small values of R have been observed experimentally for $Ri_0 \sim 5$ (see Narimousa & Fernando 1987; Stephenson & Fernando 1991).

Since we now observe, for a given Ri_0 and R, multiple forms of instability, the interesting possibility arises for resonance between the various modes of instability in the nonlinear regime. Although we do not calculate interaction coefficients, we note that for large areas of parameter space for small $R \leqslant 0.38$, linearly unstable H and T modes have wavenumbers and phase speeds satisfying the conditions for the formation

of a resonant triad (see Craik 1985). This raises the possibility that T modes may arise in these situations, even though their linear growthrate is quite small.

In §5, we interpret and discuss these results, particularly with reference to experimental evidence, and draw conclusions on their implications for the long-time evolution of an unbounded stratified shear layer.

2. Review of previous work

Taylor (1931) was the first to consider a model for the evolution of a mixed layer. He considered a piecewise linear velocity profile, forming a shear layer of depth d, which in a certain reference frame moving with the mean speed of the shear layer may be defined as

$$U(z) = \begin{cases} -\frac{1}{2}\Delta U & (z \leqslant -\frac{1}{2}d), \\ \Delta U z/d & (-\frac{1}{2}d < z < \frac{1}{2}d), \\ \frac{1}{2}\Delta U & (z \geqslant \frac{1}{2}d), \end{cases} \tag{2.1}$$

and a density field so that

$$\rho(z) = \begin{cases} \rho+\Delta\rho & (z \leqslant -\frac{1}{2}d), \\ \rho+\frac{1}{2}\Delta\rho & (-\frac{1}{2}d < z < \frac{1}{2}d), \\ \rho & (z \geqslant \frac{1}{2}d), \end{cases} \tag{2.2}$$

i.e. the intermediate mixed layer, with a density equal to the mean density of the two layers, extends across the entire depth of the shear layer. Proposing a normal mode disturbance, with wavenumber k, the phase speed (non-dimensionalized with $\frac{1}{2}\Delta U$, the maximum fluid velocity) must satisfy:

$$c^4 + \left(\frac{e^{-4\alpha}-(2\alpha-1)^2}{4\alpha^2} - 1 - \frac{Ri_0}{\alpha}\right)c^2 + \frac{Ri_0^2}{4\alpha^2}(1-e^{-4\alpha}) - \frac{Ri_0}{\alpha}\left(\frac{(2\alpha-1)+e^{-4\alpha}}{2\alpha}\right) - \left(\frac{e^{-4\alpha}-(2\alpha-1)^2}{4\alpha^2}\right) = 0, \tag{2.3}$$

which implies instability (i.e. $\mathrm{Im}(c) > 0$) for

$$\frac{2\alpha}{1+e^{-2\alpha}} < 1 + Ri_0 < \frac{2\alpha}{1-e^{-2\alpha}}, \tag{2.4}$$

where α, the non-dimensional wavenumber, is

$$\alpha \equiv \tfrac{1}{2}kd, \tag{2.5}$$

and Ri_0 is the bulk Richardson number

$$Ri_0 \equiv \frac{g\Delta\rho d}{\rho\Delta U^2}. \tag{2.6}$$

The stability boundary (i.e. the curve in (α, Ri_0) space dividing growing modes from marginally stable modes) is shown in figure 1. In this case all unstable modes have $Re(c) \equiv c_r = 0$, and thus propagate at the mean speed of the shear layer. At finite amplitude, they develop into intense regions of overturning, and lead to strong mixing of the density field. We shall refer to these modes as T (for Taylor) modes.

Taylor observed that as $Ri_0 \to \infty$, (2.4) implies that the unstable modes asymptote to the line

$$Ri_0 = 2\alpha - 1. \tag{2.7}$$

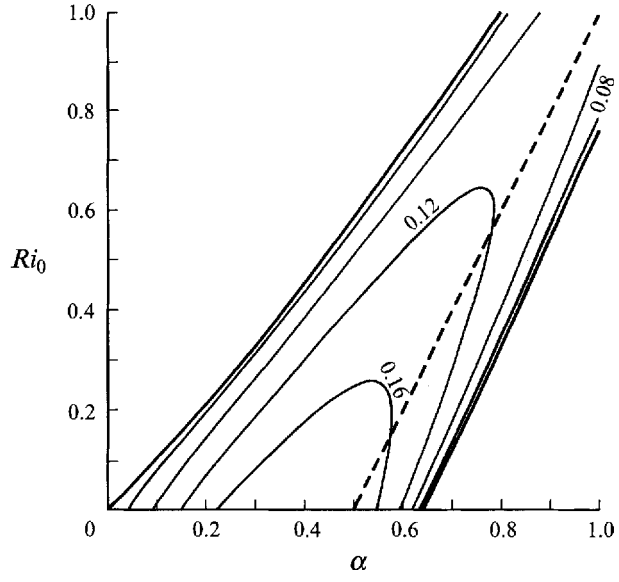

FIGURE 1. Stability boundary and asymptote (2.7) (dashed line) with contours of growthrate (at intervals 0.04) for the three-layer flow considered by Taylor (1931).

As Taylor himself noted, the large α limit corresponds to considering each interface in isolation. Considering the upper interface in isolation corresponds to analysing a (non-dimensional) flow where

$$U(z) = \begin{cases} z & (z < 1), \\ 1 & (z \geqslant 1), \end{cases} \tag{2.8}$$

$$\rho(z) = \begin{cases} \rho + \frac{1}{2}\Delta\rho & (z < 1), \\ \rho & (z \geqslant 1). \end{cases} \tag{2.9}$$

The interface supports two marginally stable internal waves with phase speeds

$$c_{1\pm} = 1 - \frac{1}{4\alpha} \pm \left(\frac{1}{16\alpha^2} + \frac{Ri_0}{2\alpha}\right)^{\frac{1}{2}}. \tag{2.10}$$

Similarly the lower interface in isolation would support two marginally stable internal waves with phase speeds

$$c_{2\pm} = -1 + \frac{1}{4\alpha} \pm \left(\frac{1}{16\alpha^2} + \frac{Ri_0}{2\alpha}\right)^{\frac{1}{2}}. \tag{2.11}$$

Requiring that the upstream propagating (relative to the ambient flow) waves of the same wavenumber α on the upper and lower interfaces have the same (zero) phase speed (i.e. $c_{1-} = c_{2+} = 0$) corresponds, in the limit of large α, to condition (2.7). (See Howard & Maslowe 1973 for a fuller discussion.) Though we have referred to these waves as internal waves, it is important to note that, since the density interface coincides with the vorticity interface, the interface will still support a wave that propagates upstream relative to the mean flow even if there is no density jump (i.e. $Ri_0 = 0$ in (2.10) and (2.11)). In this limiting case

$$c_{1-} = -c_{2+} = 1 - \frac{1}{2\alpha}, \tag{2.12}$$

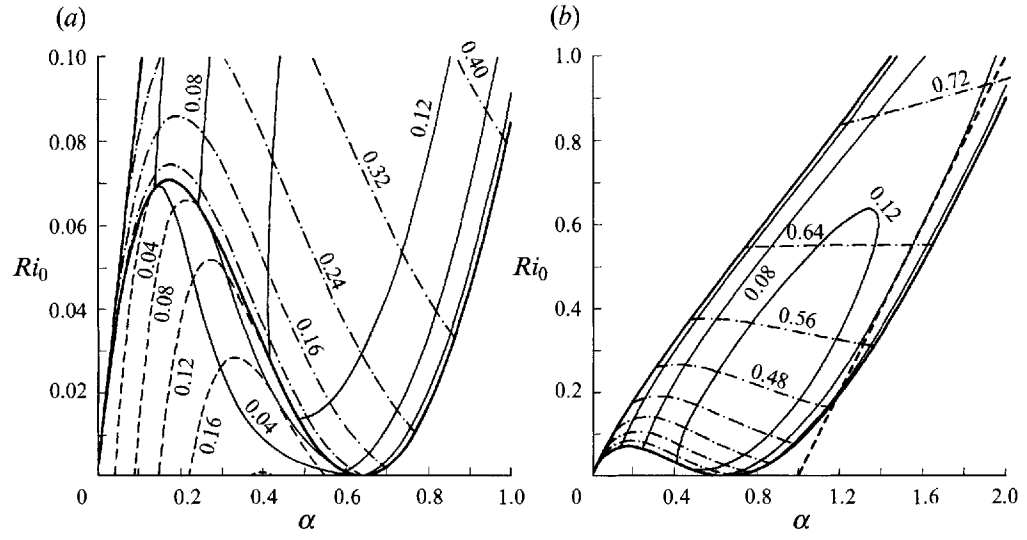

FIGURE 2. (*a*) Stability boundary, for small Ri_0 for the two-layer flow previously considered by Holmboe (1962). Below the locus with maximum at $Ri_0 = 0.07$, the solid lines and dashed lines are contours of growthrate for the two different zero phase speed instabilities, at contour intervals of 0.04. Above that locus the contours of growthrate (solid line) and phase speed (dot-dashed line at intervals 0.08) are shown for the *H* modes. (*b*) Stability boundary and asymptote (2.19) (dashed line), for large Ri_0 for the two layer flow previously considered by Holmboe (1962). Above the locus of transition to zero real phase speed instability, the contours of growthrate (solid line) and phase speed (dot-dashed line) are shown for the H modes, using the same contour intervals as in figure 2(*a*).

which, in the large α approximation, can be identified as the phase speeds of waves known as Rayleigh waves, first discussed in the context of the instability of a homogeneous shear layer (see Rayleigh 1894).

In general, (see Cairns 1979) the stability of a flow with discontinuities in the background density, velocity or vorticity fields may be qualitatively investigated by an investigation of the waves that could occur on each of the interfaces if they were totally isolated from each other. This corresponds to the large α limit considered by Taylor. Typically, for a marginally stable wave to exist on an interface, energy must either by supplied (or removed) from the flow. Cairns referred to a wave which required the input of energy as a positive energy wave, while a wave which required the removal of energy he referred to as a negative energy wave. Hayashi & Young (1987) showed that the wave energy E of an interfacial wave satisfies, in a certain reference frame,

$$E \sim -c\frac{\partial c}{\partial \alpha}. \tag{2.13}$$

For a wave to be unstable, its growth must not require any variation in the total energy of the flow. Thus, it is possible to identify instability with a resonance of two waves, with oppositely signed energy (so that their combination leaves the energy of the system unchanged) or possibly zero wave energy (typically associated with zero phase speed as in the case considered by Taylor from (2.13)) and equal phase speed and wavenumber. Thus a classification of the waves by their energy (which typically can be achieved by considering each of the interfaces in isolation) allows us to identify the possible routes to instability within a flow.

The other limiting case that throws light on our investigation is that considered by Holmboe (1962), namely a two-layer flow with no intermediate mixed layer. He

considered the piecewise linear velocity profile (2.1), but with a two-layer density distribution, with the only density interface at the midpoint of the shear layer, i.e.

$$\rho(z) = \begin{cases} \rho + \Delta\rho & (z \leqslant 0), \\ \rho & (z > 0). \end{cases} \tag{2.14}$$

In this case, the non-dimensional phase speed satisfied the equation:

$$c^4 + \left(\frac{e^{-4\alpha} - (2\alpha-1)^2}{4\alpha^2} - \frac{Ri_0}{\alpha}\right)c^2 + \frac{Ri_0}{\alpha}\left(\frac{e^{-2\alpha} + (2\alpha-1)}{2\alpha}\right)^2 = 0, \tag{2.15}$$

and the stability boundary is as shown in figure 2. In this flow, since the density interface is not coincident with a vorticity interface, we have four waves, two Rayleigh waves (one on each of the vorticity interfaces with asymptotic phase speeds given by (2.12)) and two internal waves on the density interface, such that if the sign of the phase speed of an internal wave and a Rayleigh wave is the same they have opposite wave energies. (The actual sign of the energy of a wave is not invariant with respect to changes in the frame of reference.) The asymptotic phase speed of the internal waves can be calculated by considering the following flow:

$$U(z) = z; \tag{2.16}$$

and

$$\rho(z) = \begin{cases} \rho + \Delta\rho & (z < 0), \\ \rho & (z \geqslant 0). \end{cases} \tag{2.17}$$

In the limit of large α, such an interface supports two internal waves with phase speeds

$$c_{d\pm} = \pm(Ri_0/\alpha)^{\frac{1}{2}}. \tag{2.18}$$

As is shown in figure 2(*a*), for $Ri_0 < 0.07$, (2.15) predicts that there exist two unstable modes. In the small Ri_0 case, the zero phase speed instability with larger growthrate may be identified with a stratified modification of the instability of a homogeneous shear layer discussed by Rayleigh. This arises through an interaction between the two Rayleigh waves (i.e. $c_{1-} = c_{2+} = 0$). As Holmboe describes, the effect of the density interface is to reduce the band of wavenumbers that allow this locking to take place, and also to reduce the growthrate of the mode. At finite amplitude they roll up into the well-known Kelvin–Helmholtz billows.

The zero phase speed instability with smaller growthrate can also be identified with a resonance of two interfacial waves at zero wave energy, namely the two internal waves on the density interface, with asymptotic phase speeds given by (2.18). Provided that the stratification is weak, these two modes may be sufficiently retarded by the shear to have zero phase speed, and thus resonate.

As the stratification increases, the growthrate of the second zero phase speed mode increases, until such time as the growthrate of the two unstable modes is the same. At this critical condition (see figure 2*a*) the unstable modes start to have non-zero real phase speed. Two resonances now occur simultaneously at non-zero real phase speed. First, the Rayleigh wave which is propagating upstream on the upper vorticity interface (with asymptotic phase speed c_{1-} given by (2.12)) resonates with the internal wave on the density interface that has positive real phase speed, asymptotically given by c_{d+} in (2.18). Secondly, the internal wave with negative real phase speed, asymptotically given by c_{d-} in (2.18), resonates with the Rayleigh wave on the lower vorticity interface (with asymptotic phase speed c_{2+} given by (2.12)). These resonances occur as the phase speeds of the internal waves can no longer be sufficiently strongly

retarded by the shear to bring them to zero. As can be seen in figure 2(*b*), at large wavenumber α and Ri_0 the region of instability asymptotes to the line

$$Ri_0 = \alpha - 1. \tag{2.19}$$

Analogously to Taylor's flow, $c_{1-} = c_{a+} = -c_{a-} = -c_{2+}$ implies (2.19).

Thus for $Ri_0 > 0.07$ there exist pairs of oscillatory modes with equal and opposite real phase speeds. (In fact, owing to the symmetry of biquadratic equations there also exist two decaying modes with equal and opposite real phase speeds.) At finite amplitude, numerical calculations (see Smyth *et al.* 1988) demonstrate that these modes develop regions of strong vorticity (and overturning) in the vicinity of the critical layer (where the phase speed of the mode corresponds to the background velocity of the flow). Two such regions of vorticity, one above and one below the interface lead to the pairs of cusped propagating waveforms that have subsequently been observed both experimentally (Browand & Winant 1973) and numerically (Smyth *et al.* 1988), and their combination is referred to as a Holmboe or H mode. At finite amplitude, an H mode consists of two counter-propagating cusped waves at the density interface, that occasionally wisp off small quantities of fluid from their peaks, owing to the region of vorticity in the vicinity of the upper critical layer attempting to lift the denser fluid upwards, and the lower region of vorticity attempting to pull the lighter fluid downwards. (This may be the mechanism for the generation of vortices above and below the density interface for intermediate Ri_0 reported by Narimousa & Fernando (1987) as the main mechanism for mixing for moderate to strong stratifications.) As Ri_0 increases, the phase speed of the oscillatory modes, and hence the distance of the regions of intense vorticity from the interface increases while the growthrate of the mode decreases (after a small initial increase for $Ri_0 \leqslant 0.2$). Thus the amount of wisping, and hence mixing will tend to decrease. Indeed, in a two-layer system, Holmboe modes are generally associated with much less mixing than the Kelvin–Helmholtz billows.

Thus, when the depth of the layer of intermediate density precisely matches that of the shear layer, the flow is unstable to T modes, while if there is no region of intermediate density, the flow is dominated by H mode oscillatory instabilities.

3. Derivation of governing equations

We consider the following flow, as depicted in figure 3. We assume that the fluid is inviscid, i.e. the kinematic viscosity $\nu = 0$. The fluid is stratified in a stepwise fashion into three layers, with densities $\rho, \rho + \frac{1}{2}\Delta\rho$, and $\rho + \Delta\rho$ respectively. The central region is of arbitrary depth δ relative to the depth of the shear layer d, with midpoint coincident with that of the shear layer. For the sake of simplicity we restrict our attention to this symmetric situation. We define the ratio, R of the intermediate layer depth and the shear layer depth as

$$R = \delta/d. \tag{3.1}$$

The velocity profile is piecewise linear, defined by (2.1), and the density field is given by

$$\rho(z) = \begin{cases} \rho + \Delta\rho & (z \leqslant -\frac{1}{2}Rd), \\ \rho + \frac{1}{2}\Delta\rho & (-\frac{1}{2}Rd < z < \frac{1}{2}Rd), \\ \rho & (z \geqslant \frac{1}{2}Rd). \end{cases} \tag{3.2}$$

Since we are ultimately interested in interpreting our results in terms of waves on the various interfaces, we follow the technique of Holmboe (1962) and derive evolution

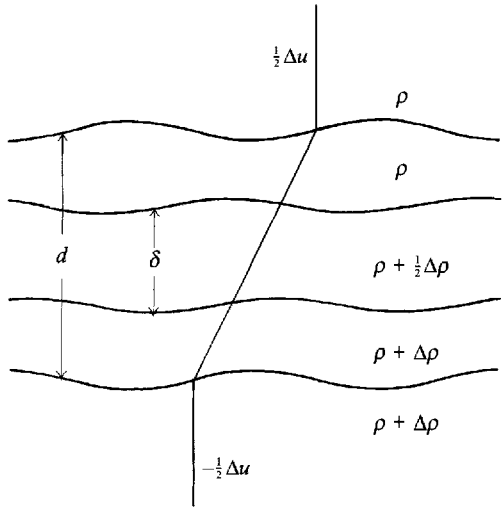

FIGURE 3. Schematic diagram of the model flow considered in the text.

equations for each of the interfaces. This is, of course, equivalent to the classical approach of Rayleigh (1894) matching pressure and vertical disturbance across the interfaces.

Following Holmboe, we consider the vorticity field as being made up of two components. The first, which we call the dynamic vorticity of the system, arises from the effect of the steps in the density distribution. This vorticity is constantly changing on the parcels of fluid on the density interfaces owing to baroclinic effects. Remembering that the ambient velocity distribution is a function of z alone, the cross-stream (i.e. y) component of the vorticity equation may be written as, following Hoiland (1948),

$$\frac{\mathrm{D}}{\mathrm{D}t}\left(\frac{\partial u}{\partial z}\right) = \left(\frac{g\Delta\rho}{\rho}\frac{\partial z_T}{\partial x}\right)\delta(z - z_T), \tag{3.3}$$

where $\delta(x)$ is the Dirac δ-function, z_T is the perturbation displacement of a density interface with density jump $\Delta\rho$ across the interface, u is the total velocity in the along stream (x) direction (i.e. the sum of the ambient and perturbation velocities or $\bar{U}+u'$), and $\mathrm{D}/\mathrm{D}t$ is the convective derivative, defined as

$$\frac{\mathrm{D}}{\mathrm{D}t} = \frac{\partial}{\partial t} + \boldsymbol{u}\cdot\boldsymbol{\nabla},$$

where $\mathbf{u}$ is the vector form of the total velocity. In the linear regime, we see that at some height z_a, the convective derivative becomes

$$\frac{\mathrm{D}}{\mathrm{D}t} \equiv \frac{\partial}{\partial t} + \bar{U}(z_a)\frac{\partial}{\partial x}. \tag{3.4}$$

We assume that $z_T \sim \exp(\mathrm{i}kx)$, i.e. the perturbation is sinusoidal with wavelength $2\pi/k$. Thus if we integrate (3.3) over an arbitrarily small region in the vicinity of the density interface, we obtain

$$\frac{\mathrm{D}}{\mathrm{D}t}(u^+ - u^-)_T = \left(\frac{g\Delta\rho}{\rho}\frac{\partial z_T}{\partial x}\right), \tag{3.5}$$

where
$$u^+ = \lim_{z \to z_T^+} u, \tag{3.6}$$

$$u^- = \lim_{z \to z_T^-} u. \tag{3.7}$$

Such a density interface sets up a Laplacian velocity field away from the interface, which may be represented by a streamfunction

$$\psi_T(x, z, t) = \hat{\psi}_T(z)\, \psi'_T(x, t). \tag{3.8}$$

Without loss of generality we may transform to a frame of reference, where the density interface is at $z = 0$, if the fluid is unperturbed. Thus, since the fluid is of constant density away from $z = 0$,

$$\psi_T = \psi'_T e^{-k|z|}. \tag{3.9}$$

Therefore
$$u \equiv -\frac{\partial \psi_T}{\partial z}, \tag{3.10}$$

$$= -\psi'_T \frac{d\hat{\psi}_T}{dz}, \tag{3.11}$$

$$u^{\pm} = \pm k \psi'_T, \tag{3.12}$$

and
$$\frac{D}{Dt}\psi_T = \frac{g'}{2k}\frac{\partial z_T}{\partial x}, \tag{3.13}$$

where
$$g' = \frac{g\Delta\rho}{\rho}, \tag{3.14}$$

is, as usual, the reduced gravity. We note that (3.13) is a totally local equation, i.e. the dynamic vorticity associated with a certain density interface is determined by the evolution of that density interface alone. Locally at that interface, since ψ_T is decomposable into normal modes we know (see Batchelor 1967) that the dynamic vorticity ω_D is linearly related to, and has the same sign as, ψ_T. Thus, henceforth, when we wish to discuss the behaviour of the dynamic vorticity, we shall discuss the behaviour of ψ_T. Also we see that away from its rest value z_T decays exponentially in the z-direction, owing to the constant density away from $z = 0$.

The other component of the vorticity field is known as the kinematic vorticity and is due to the deformation of vorticity interfaces at the boundaries of the shear layer. In this case, the vorticity of the fluid parcels is conserved. Such deformations ($\sim \exp(ikx)$ again) will also set up a Laplacian velocity in the surrounding fluid, with an associated stream function

$$\psi_S(x, z, t) = \hat{\psi}_S(z)\, \psi'_S(x, t). \tag{3.15}$$

If we let z_S denote the deformation of the boundary of the shear layer, application of Stokes' theorem yields

$$\psi_S(x, z, t) = \pm\left(\frac{\Delta U}{2kd}\right) z_S, \tag{3.16}$$

the plus and minus signs being dependent on whether we are considering the upper or

lower vorticity interface, respectively. Since we have irrotational flow outside the shear layer, the Laplacian nature of the velocity field once again implies that away from its rest value, z_S decays exponentially with vertical distance.

Now let us consider the geometry of figure 3. There are six unknowns, namely the perturbation disturbances of the upper and lower vorticity interfaces (henceforth labelled z_1 and z_2, respectively), the perturbation disturbances of the upper and lower density interfaces, (z_u and z_l), and the streamfunctions associated with the dynamic vorticity at the upper and lower density interfaces (ψ_u and ψ_l). The evolution of a specific perturbation disturbance is coupled to the evolution of the other disturbances. We note that the effect of any perturbation decays exponentially the distance, and that by our choice of coordinate system, positive vorticity corresponds to a clockwise circulation, so the shear layer, in the absence of density interfaces, would correspond to a region of constant positive vorticity.

Combining the evolution equations of the disturbances, with the dynamic vorticity equations, and remembering that the density interfaces now have density jumps of $\frac{1}{2}\Delta\rho$ associated with them, we obtain the following coupled system of six differential equations

$$\frac{\mathrm{D}}{\mathrm{D}t}\psi_u = \frac{Ri_0}{kd}\left(\frac{\Delta U}{2}\right)^2 \frac{\partial z_u}{\partial x}, \tag{3.17}$$

$$\frac{\mathrm{D}}{\mathrm{D}t}\psi_l = \frac{Ri_0}{kd}\left(\frac{\Delta U}{2}\right)^2 \frac{\partial z_l}{\partial x}, \tag{3.18}$$

$$\frac{\mathrm{D}}{\mathrm{D}t}z_u = \frac{\partial}{\partial x}\left[\psi_u + \exp(-k\delta)\,\psi_l + \frac{\Delta U \exp(-\frac{1}{2}k(d-\delta))}{2kd}(z_1 - \exp(-k\delta)\,z_2)\right], \tag{3.19}$$

$$\frac{\mathrm{D}}{\mathrm{D}t}z_l = \frac{\partial}{\partial x}\left[\psi_l + \exp(-k\delta)\,\psi_u + \frac{\Delta U \exp(-\frac{1}{2}k(d+\delta))}{2kd}(z_1 - \exp(k\delta)\,z_2)\right], \tag{3.20}$$

$$\frac{\mathrm{D}}{\mathrm{D}t}z_1 = \frac{\partial}{\partial x}\left[\frac{\Delta U}{2kd}(z_1 - \exp(-kd)\,z_2) + \exp(-\tfrac{1}{2}k(d-\delta))\,(\psi_u + \exp(-k\delta)\,\psi_l)\right], \tag{3.21}$$

$$\frac{\mathrm{D}}{\mathrm{D}t}z_2 = \frac{\partial}{\partial x}\left[\frac{\Delta U}{2kd}(-z_2 + \exp(-kd)\,z_1) + \exp(-\tfrac{1}{2}k(d+\delta))\,(\psi_u + \exp(k\delta)\,\psi_l)\right]. \tag{3.22}$$

We note that this model requires $R \leqslant 1$, i.e. the density varying region must be embedded in the shear layer.

We now non-dimensionalize all quantities with respect to the intrinsic scales of distance and time of the system, i.e. $\frac{1}{2}d$, the halfdepth of the shear layer, and $\frac{1}{2}\Delta U$, the maximum absolute value of velocity. Thus if asterisks denote dimensional quantities, we transform into non-dimensional variables thus:

$$\left.\begin{aligned} z^* = \tfrac{1}{2}d^* z, \quad t^* = \frac{td^*}{\Delta U^*}, \quad x^* = \tfrac{1}{2}xd^*, \\ R = \frac{\delta^*}{d^*}, \quad \alpha = \tfrac{1}{2}d^*k^*, \quad \psi^* = \tfrac{1}{4}\Delta U^* d^* \psi. \end{aligned}\right\} \tag{3.23}$$

There are also clear symmetries in these equations, and so we now consider (3.17)–(3.22) in terms of $z_1 \pm z_2$, $z_u \pm z_l$ and $\psi_u \pm \psi_l$, i.e.

$$\frac{\partial}{\partial t}(\psi_u \pm \psi_l) = \frac{\partial}{\partial x}\left(\frac{Ri_0}{2\alpha}(z_u \pm z_l) - R(\psi_u \mp \psi_l)\right), \tag{3.24, 3.25}$$

$$\frac{\partial}{\partial t}(z_u \pm z_l) = \frac{\partial}{\partial x}\left([1 \pm \mathrm{e}^{-2\alpha R}]\left[\psi_u \pm \psi_l + \frac{\mathrm{e}^{-\alpha(1-R)}}{2\alpha}(z_1 \mp z_2)\right] - R[z_u \mp z_l]\right), \tag{3.26, 3.27}$$

$$\frac{\partial}{\partial t}(z_1 \pm z_2) = \frac{\partial}{\partial x}\left(\frac{[1 - 2\alpha \pm \mathrm{e}^{-2\alpha}]}{2\alpha}(z_1 \mp z_2) + \mathrm{e}^{-\alpha}[\mathrm{e}^{\alpha R} \pm \mathrm{e}^{-\alpha R}](\psi_u \pm \psi_l)\right). \tag{3.28, 3.29}$$

With this non-dimensionalization, we can eliminate from (3.24)–(3.29) all variables except for z_1–z_2, the relative disturbance of the shear layer. We postulate the classical normal mode form for z_1–z_2, i.e.

$$z_1^* - z_2^* \sim \exp(\mathrm{i}k^*[x^* - c^*t^*]), \tag{3.30}$$

where

$$c^* = \tfrac{1}{2}c\Delta U \tag{3.31}$$

is the dimensional phase speed of the disturbance. In general c can be complex, and we write

$$c \equiv c_r + \mathrm{i}c_i, \quad (z_1 - z_2) \sim \exp\alpha(c_i t + \mathrm{i}[x - c_r t]). \tag{3.32}$$

The flow is unstable if $c_i > 0$, with growthrate αc_i. With this form for $z_1 - z_2$ (3.24)–(3.29) reduce to a bicubic eigenvalue equation in c

$$c^6 + a_2 c^4 + a_4 c^2 + a_6 = 0, \tag{3.33}$$

where

$$a_2 = -2R^2 - \frac{Ri_0}{\alpha} + \frac{\mathrm{e}^{-4\alpha} - (2\alpha - 1)^2}{4\alpha^2}, \tag{3.34}$$

$$a_4 = -2R^2\left(\frac{\mathrm{e}^{-4\alpha} - (2\alpha-1)^2}{4\alpha^2}\right) + \frac{Ri_0}{\alpha}\left(\frac{\mathrm{e}^{-4\alpha} + (2\alpha-1)^2}{4\alpha^2}\right) + \left(R^2 - \frac{Ri_0}{2\alpha}\right)^2 - \frac{Ri_0^2\,\mathrm{e}^{-4\alpha R}}{4\alpha^2} + \frac{Ri_0\,\mathrm{e}^{-2\alpha}}{\alpha^3}(2\alpha R \sinh 2\alpha R + \tfrac{1}{2}(2\alpha - 1)\cosh 2\alpha R), \tag{3.35}$$

$$a_6 = \left(\frac{\mathrm{e}^{-4\alpha} - (2\alpha-1)^2}{4\alpha^2}\right)\left(R^4 + \frac{Ri_0^2}{4\alpha^2}\right) + \frac{Ri_0^2\,\mathrm{e}^{-4\alpha R}}{4\alpha^2}\left(\frac{(2\alpha-1)^2 - \mathrm{e}^{4\alpha(2R-1)}}{4\alpha^2}\right) + \frac{Ri_0 R^2}{\alpha}\left(\frac{\mathrm{e}^{-4\alpha} + (2\alpha-1)^2}{4\alpha^2}\right) + \frac{Ri_0\,\mathrm{e}^{-2\alpha}(2\alpha-1)}{4\alpha^4}(2\alpha R^2 \cosh 2\alpha R - Ri_0 \sinh 2\alpha R). \tag{3.36}$$

In the limits $R = 0$ and $R = 1$, (3.33) reduces, upon division by $(c^2 - R^2)$, to the results of Holmboe (2.15) and Taylor (2.3), respectively.

4. Variation of instability properties with R

We now turn our attention to the arbitrary R case, and consider solutions of (3.33). Although the roots of (3.33) can be written formally in an explicit fashion, using Cardano's formula, the form calculated was too complex to reward direct analysis of the general result, owing to the dependence on α, Ri_0, and R. However, if we restrict our attention to attempting to finding general expressions for the transitions from marginal stability to instability, significant progress can be made.

Also, if we first consider the large α limit of this flow, we know that the upper and lower vorticity interfaces, for $R \neq 1$ support Rayleigh waves with asymptotic phase speeds given by (2.12), just as in the two-layer case discussed by Holmboe. However, there are now two density interfaces within the flow, each of which support two internal waves.

Consider the behaviour of a density interface at $z = R$ in an infinite region of constant shear, i.e.

$$U(z) = z \quad (-\infty < z < \infty), \tag{4.1}$$

and

$$\rho(z) = \begin{cases} \rho + \frac{1}{2}\Delta\rho & (z < R), \\ \rho & (z \geqslant R). \end{cases} \tag{4.2}$$

In this case, the complete system is described by two equations for the streamfunction ψ_u, and the interfacial displacement z_u thus

$$\frac{\partial}{\partial t}\psi_u = \frac{\partial}{\partial x}\left(\frac{Ri_0}{2\alpha} z_u - R\psi_u\right), \tag{4.3}$$

$$\frac{\partial}{\partial t} z_u = \frac{\partial}{\partial x}(-Rz_u + \psi_u), \tag{4.4}$$

which, for normal mode disturbances, imply that

$$(c-R)^2 - \frac{Ri_0}{2\alpha} = 0. \tag{4.5}$$

So, considering the upper density interface in isolation, we can see that it supports two internal waves

$$c_{u\pm} = R \pm \left(\frac{Ri_0}{2\alpha}\right)^{\frac{1}{2}}. \tag{4.6}$$

Similarly, the lower density interface considered in isolation also supports two internal waves

$$c_{l\pm} = -R \pm \left(\frac{Ri_0}{2\alpha}\right)^{\frac{1}{2}}. \tag{4.7}$$

4.1. *Zero real phase speed instability: large α*

In general, a transition to or from instability for a region of zero real phase speed instability occurs when $c = 0$ is a double root of (3.33), which corresponds to

$$a_6 = 0. \tag{4.8}$$

Equation (4.8), from (3.36), can be interpreted as a quadratic equation in Ri_0 for given R and α, which, provided $R \neq 0$, is satisfied when

$$Ri_0 = \left(\frac{2\alpha R^2}{1-e^{-4\alpha R}}\right)\left(\frac{e^{-4\alpha} + (2\alpha-1)^2 + 2(2\alpha-1)e^{-2\alpha}\cosh 2\alpha R}{[(2\alpha-1)+e^{-2\alpha(1-R)}]^2} \pm e^{-2\alpha R}\right), \tag{4.9a}$$

or, equivalently

$$Ri_0 = \frac{2\alpha R^2[(2\alpha-1) \pm e^{-2\alpha}]}{[1 \mp e^{-2\alpha R}][(2\alpha-1)+e^{-2\alpha(1-R)}]}. \tag{4.9b}$$

When $R = 1$, (4.9) reduces to

$$Ri_0 = \frac{2\alpha}{1 \mp e^{-2\alpha}} - 1, \tag{4.10}$$

which are just the critical limits of (2.4). Also (4.10) shows that, when $Ri_0 = 0$, we may recover the result of Rayleigh (1894). Provided that

$$e^{-2\alpha} < 2\alpha - 1, \tag{4.11}$$

and hence the flow is stable when $Ri_0 = 0$, (4.9) implies that there are two real positive values of Ri_0 where (3.33) has a double root, $c = 0$. Between these values it is possible to verify that $a_6 > 0$, and hence that $c = \pm ic_1$ for some c_1, and hence that the flow is unstable to a disturbance with zero real phase speed.

If we wish to identify the interaction of interfacial waves that leads to this instability, it is instructive, as before, to consider the large α limit. In that case, (4.9) reduces to

$$Ri_0 = 2\alpha R^2. \tag{4.12}$$

Condition (4.12) corresponds to $c_{u-} = c_{l+} = 0$, (see (4.6) and (4.7)) and so we may identify this branch of instability with a resonance between the internal waves on each of the density interfaces which are propagating upstream relative to the background flow. This is the arbitrary R analogue of the modes discussed by Taylor, and thus we refer to them as T modes. It is of interest to note that, when $R \neq 1$, these T modes arise through an interaction of 'pure' internal waves, rather than the combined internal and Rayleigh waves (defined asymptotically by (2.11)) considered by Taylor in the $R = 1$ case.

4.2. *Non-zero real phase speed instability: large α*

Of course, in general, the flow may be unstable to disturbances with non-zero real phase speed. In that case, owing to the symmetry of the system, at the transition to oscillatory instability the eigenvalues of the system must consist of a pair of double roots $c = \pm c_2$, and so c^2 must have a double root. For the cubic equation of c^2, i.e. (3.33), it is well known that the equation has a double root if and only if the discriminant D,

$$D \equiv \frac{a_4^2}{27}(a_4 - \tfrac{1}{4}a_2^2) + \tfrac{1}{4}a_6^2 + \tfrac{1}{3}a_2 a_6(\tfrac{1}{9}a_2^2 - \tfrac{1}{2}a_4) = 0. \tag{4.13}$$

By inspection of (3.34)–(3.36), since a_2 is first order in Ri_0, while a_4 and a_6 are second order in Ri_0, (4.13) defines a sextic equation in Ri_0 for given α and R. The derivation of this equation is straightforward, though a little laborious. It transpires that the constant term is always zero, and hence (4.13) reduces to a quintic in Ri_0,

$$b_0 Ri_0^5 + b_1 Ri_0^4 + b_2 Ri_0^3 + b_3 Ri_0^2 + b_4 Ri_0 + b_5 = 0, \tag{4.14}$$

where the b_i are given in Appendix A. Equation (4.14) implies that there are at most five non-zero transitions to or from oscillatory instability at non-zero Ri_0 for given α and R.

Guided by the relative complexity of the two-layer results of Holmboe (1962) at small Ri_0 and α, we initially investigate the situation for large α. For all $R \neq 1$, for sufficiently large α, four of the roots of (4.14) are real and positive, and the fifth is negative. Typically, the four positive roots subdivide further into two pairs, one at appreciably larger α than the other. In figure 4 we show the four positive roots of (4.14) (solid lines) and the two roots of (4.8) given by (4.9) (dotted lines) for various α for

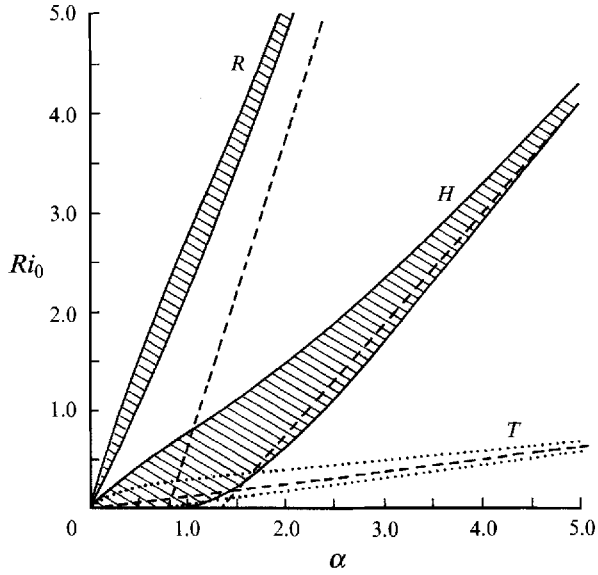

FIGURE 4. Roots of (4.14) (solid lines) and (4.8) (dotted lines) for a three-layer flow with $R = 0.25$. The dashed lines denote asymptotic conditions for resonance of the various interfacial waves which lead to instability. Oscillatory instability is predicted in the shaded areas, while zero real phase speed instability occurs for flows with parameters defining points between the two dotted lines.

$R = 0.25$. For values of Ri_0 in the shaded areas, $D > 0$, and hence (3.33) has two pairs of complex conjugate roots $c = c_r \pm ic_i$, and $c = -c_r \pm ic_i$. Thus, for general R, this flow has two, distinct regions of oscillatory instability. Between the dotted lines, the flow exhibits instability of the T mode type.

As is also shown in figure 4 (by dashed lines), the values of Ri_0 defining the three regions of instability have well-defined asymptotes as α increases. For given Ri_0, the region at largest α is well predicted by (4.12), and can be identified as the T mode. The region at intermediate α is tending to

$$Ri_0 = 2(1-R)(\alpha(1-R)-1), \tag{4.15}$$

while the region at smallest α is tending to

$$Ri_0 = 2(1+R)(\alpha(1+R)-1). \tag{4.16}$$

To identify the interfacial wave resonances which lead to these instabilities (and hence enable us to arrive at (4.15) and (4.16) in a consistent manner) it is necessary to take into account waves on the vorticity interfaces.

By symmetry, we may restrict our discussion to the behaviour of the stable waves in the upper half plane. For sufficiently large α and Ri_0 c_{1-} (from (2.12)), c_{u+} (from (4.6)) and c_{l+} (from (4.7)) are all greater than zero. However, owing to the differing dependence on α, (2.13) predicts that c_{u+} and c_{l+} have wave energy opposite in sign to that of c_{1-}. So we expect instability if their phase speeds are equal at the same value of α. In the limit of large α, $c_{1-} = c_{u+}$ implies (4.15), and $c_{1-} = c_{l+}$ implies (4.16). Thus the region of instability in figure 4 at intermediate α arises through a resonance between the Rayleigh wave and the downstream propagating internal wave on the nearer density interface. This is a three-layer analogue of the behaviour described in the introduction for the Holmboe waves in a two-layer flow, and so we identify this particular branch as an H mode branch.

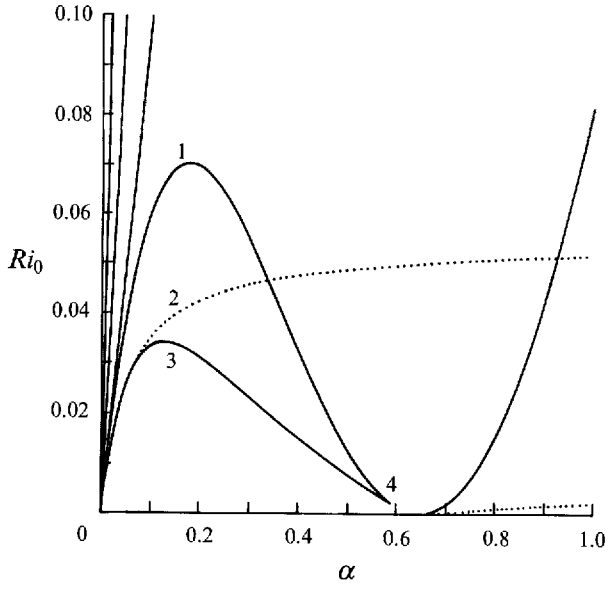

FIGURE 5. Roots of (4.14) and (4.8) for a three-layer flow with $R = 0.05$. See text for explanations of the marked transitions 1–4.

On the other hand, the region of instability in figure 4 at smallest α arises through a resonance between the Rayleigh wave and the upstream propagating internal wave on the further density interface. This has no analogue in either the two-layer flow of Holmboe or the three-layer flow of Taylor, and implicitly requires the existence of an intermediate layer. This branch consists of the R modes mentioned in §1.

4.3. *Instability at small* α

At small α, in particular if R is also small or close to 1, the effect of the various interfaces upon each other can no longer be neglected. This manifests itself in the behaviour of the roots of (4.14), which for small α no longer simply delineate two branches of instability. As an example, let us consider a flow where $R = 0.05$, for wavenumbers between 0 and 1. In figure 5, we plot the roots of Ri_0 corresponding both to transitions to and from oscillatory instability (solid lines) and transitions to and from zero phase speed instability (dotted line). For $0 < \alpha < 0.59$, (4.14) has five real and positive roots, for $0.59 < \alpha < 0.63$, (4.14) has two complex roots and three real roots, for $0.63 < \alpha < 0.66$, (4.14) has three positive and two negative real roots, while for $\alpha > 0.66$, (4.14) has, as previously discussed, four positive real roots, and one negative real root.

In figure 6 we plot the evolution of the phase speed (solid lines) and growthrate (dashed lines) for roots of the eigenvalue equation (3.33) against Ri_0 for $\alpha = 0.15$. It is possible to draw analogies with the behaviour at small Ri_0 for the $R = 0$ case. As we reduce Ri_0 we see in both cases a transition (marked at point 1 on figure 5) from H mode type behaviour, and hence a resonance between the Rayleigh wave on a vorticity interface and the internal wave on the nearer (or only) density interface which would, if the density interface were isolated, propagate downstream, to two zero real phase speed instabilities. One of these is a resonance between the two Rayleigh waves, the other being the two (nominally downstream propagating) internal waves. The resonance between the two Rayleigh waves continues to occur as Ri_0 decreases, with

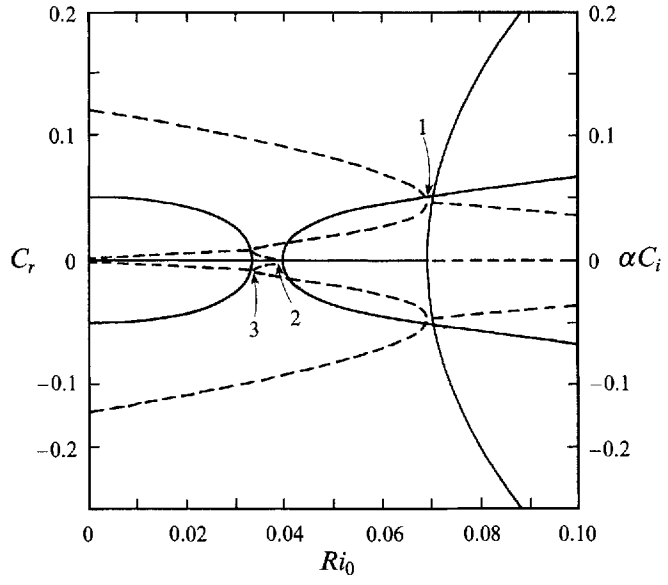

FIGURE 6. Evolution of the phase speed (solid lines) and growthrate (dashed lines) of the various modes, solutions of (3.33), as Ri_0 is varied for $\alpha = 0.15$, $R = 0.05$.

ever increasing growthrate, which is to be expected since this is an instability that is essentially homogeneous in character. The internal wave resonance has decreasing growthrate as Ri_0 is decreased.

However, the internal wave resonance does not retain its behaviour as Ri_0 is decreased. At point 2 in figure 5, as we pass into the region of T mode type instability, the (nominally) upstream propagating internal waves on each of the density interfaces resonate. All three (unstable) modes now have zero real phase speed. At point 3 on figure 5, this last T mode type resonance has the same growthrate as the other internal wave resonance which has been decreasing in magnitude of growthrate. Here the behaviour changes character. For Ri_0 below this point, there is a resonance locally between the internal waves on each interface. This local resonance has non-zero real phase speed, and has no analogue in the $R = 0$ case studied by Holmboe (1962). Since its mechanism for growth is different from that of the Holmboe instability, although it has non-zero real phase speed, we will not classify it as an H mode, but rather as an L (for local) mode. As can be seen from figure 6, for both the L mode, and the zero real phase speed instability between points 1 and 3, the growthrate increases with Ri_0, thus raising the possibility that these modes are subject to primary three-dimensional instabilities. However, the Rayleigh wave interaction always has appreciably larger growthrate, and it can be verified that all primary instabilities are two-dimensional in character.

As regards the variation of these properties with R, the curve defining the transition from H mode type behaviour to that of Rayleigh wave instability varies little as R increases from zero. This is unsurprising, since the retarding effect of the two (relatively close together) density interfaces on the Rayleigh waves on the vorticity interfaces is quite similar to the effect of one (notional) density interface at the midpoint between the two density interfaces (the situation studied by Holmboe). The curve defining the extent of the region L mode instability lifts off the wavenumber axis as R increases, as the possibility of local interaction on a density interface increases. On the other hand, as R increases, the interaction between the Rayleigh waves and the internal waves on

the nearer density interface becomes stronger (i.e. the H mode resonance), until the Rayleigh wave interaction and the L mode interaction become impossible. In this situation, as Ri_0 decreases, the phase speed of the H mode never goes to zero, and thus it is never possible for a transfer of resonance with the waves that make up the T mode. For $R = 0.05$ this takes place at point 4 in figure 5. As R gets larger this point moves to smaller and smaller wavenumber.

An associated interesting observation is that, as R increases, H mode type instability is predicted for arbitrarily small Ri_0 for $\alpha > 0.64$, i.e. the region of stability for a homogeneous flow. Indeed, as R increases, the value α_{crit} at which (4.14) has a root at $Ri_0 = 0$, progressively increases with a well-defined relationship to R, namely

$$R^2 = \frac{(2\alpha_{crit}-1)^2 - e^{-4\alpha_{crit}}}{4\alpha_{crit}^2}. \tag{4.17}$$

For flows where $R \sim 1$, (4.17) approaches

$$R \sim \frac{2\alpha_{crit}-1}{2\alpha_{crit}}, \tag{4.18}$$

or equivalently

$$\alpha_{crit} \sim \frac{1}{2(1-R)}. \tag{4.19}$$

As has already been mentioned, transitions to and from H mode type instability correspond to c^2 having a double root in (3.33). Also, H mode instability corresponds to a resonance between the Rayleigh waves and the internal waves on the density interfaces. When $Ri_0 \to 0$, (3.33) becomes

$$c^6 + \left[\frac{e^{-4\alpha}-(2\alpha-1)^2}{4\alpha^2} - 2R^2\right]c^4 + \left[R^4 - 2R^2\left(\frac{e^{-4\alpha}-(2\alpha-1)^2}{4\alpha^2}\right)\right]c^2 + R^4\left(\frac{e^{-4\alpha}-(2\alpha-1)^2}{4\alpha^2}\right) = 0. \tag{4.20}$$

Thus, the condition that the (notional) internal waves, and the Rayleigh waves on the vorticity interfaces have the same phase speeds is simply (4.17).

When α is close to α_{crit}, as is shown in Appendix B, b_5 in (4.14) is positive (negative) for $\alpha < (>)\alpha_{crit}$. Thus for small Ri_0, the discriminant of the eigenvalue equation (3.33) is positive (negative) for positive Ri_0, and hence there do (not) exist two waves with non-zero real phase speed and positive growth for arbitrarily small positive Ri_0, and at that particular wavenumber, for negative but small magnitude Ri_0 the flow is stable (unstable). This existence of a region of statically unstable (α, Ri_0) space where the flow is marginally stable owing to the effects of the shear has been noted before for an asymmetric two-layer shear flow (see Lawrence *et al.* 1991), and is well known in situations of convective flow. Of more interest to us is that, for arbitrarily small (positive) Ri_0, the flow becomes unstable to H mode type disturbances, raising once again the possibility that these H modes are subject to primary three-dimensional instabilities.

4.4. *Properties of the growing modes*

Though we can identify the possible growth mechanisms and the asymptotic behaviour of the system by simple consideration of the various interfaces, it is necessary to solve (3.33) directly to obtain the full picture for the behaviour of the system under consideration.

Of particular interest is the question of whether a mode, travelling at an angle to the mean flow is predicted to be the most unstable possible mode for a given set of flow parameters (in the sense of having the largest growthrate) and thus is predicted to dominate the evolution of the flow.

As is discussed by Smyth *et al.* (1988), we consider a normal mode $\exp[\mathrm{i}(\alpha_x x + \alpha_y y - |\boldsymbol{\alpha}|ct)]$ (i.e. with wavenumber vector $\boldsymbol{\alpha} = (\alpha_x, \alpha_y, 0)$ and (complex) phase speed c) which makes an angle ϕ with the background flow, where

$$\phi \equiv \cos^{-1}\left[\frac{\alpha_x}{(\alpha_x^2+\alpha_y^2)^{\frac{1}{2}}}\right]$$

$$= \cos^{-1}\left[\frac{\alpha_x}{|\boldsymbol{\alpha}|}\right]. \tag{4.21}$$

Also, we define the (complex) growthrate σ of a mode as

$$\sigma = \sigma_r + \mathrm{i}\sigma_i \equiv \mathrm{i}\,|\boldsymbol{\alpha}|\, c. \tag{4.22}$$

The normal mode can only extract energy (through the Reynolds stress) from the component of the background velocity parallel to the wavenumber vector, α, namely $\bar{U}\cos\phi$. Similarly, its growthrate in this direction is reduced by a factor $\alpha_x/|\boldsymbol{\alpha}|$, i.e. $\cos\phi$. Thus, this three-dimensional mode has an 'equivalent' two-dimensional mode with complex phase speed $c\cos\phi$, in a background flow with velocity $\bar{U}\cos\phi$. Since, from (2.6), Ri_0 involves the square of the ambient velocity, this equivalent background flow has $Ri_0/\cos^2\phi$.

In general, the growthrate of a mode is a function of the Richardson number pertaining in its background flow, as well as the wavenumber of the mode. From the above results, we see that the growthrate of the three-dimensional mode is related to that of its equivalent two-dimensional mode by the following relationship, as quoted by Smyth *et al.* (1988).

$$\sigma(\boldsymbol{\alpha}, \phi, Ri_0) = \sigma(\alpha_x/\cos\phi,\, Ri_0/\cos^2\phi)\cos\phi. \tag{4.23}$$

(We note that $\alpha_x/\cos\phi = |\boldsymbol{\alpha}|$). We can thus calculate the growthrate of the mode moving at an angle to the mean flow in terms of a two-dimensional mode in an equivalent flow with greater Ri_0. However, owing to the factor $\cos\phi$ multiplying the growthrate on the right-hand side, it is not sufficient to establish that the growthrate of a particular type of mode increases as Ri_0 increases to prove the existence of a primary three-dimensional instability, as suggested by Browand & Winant (1973) and Lawrence *et al.* (1991). Nevertheless, simple conditions can be derived involving Ri_0.

From (4.23), we expect to see a three-dimensional instability propagating at an angle ϕ if and only if the maximal (with respect to wavenumber) growthrate at Ri_0 (which we shall denote as $\sigma_{r\,max}\,(Ri_0)$) is less than $\sigma_{r\,max}\,(Ri_0/\cos^2\phi)\cos\phi$. Thus we require, on squaring (4.23) then dividing across by Ri_0,

$$\frac{\sigma_{r\,max}^2(Ri_0)}{Ri_0} < \frac{\sigma_{r\,max}^2(Ri_0/\cos^2\phi)}{Ri_0/\cos^2\phi}. \tag{4.24}$$

Thus three-dimensional modes grow most strongly at Richardson number $Ri_0 = Ri_1$ say, if and only if

$$\frac{\mathrm{d}}{\mathrm{d}s}\left(\frac{\sigma_{r\,max}}{Ri_0^{\frac{1}{2}}}\right)\bigg|_{Ri_0=Ri_1} > 0, \tag{4.25}$$

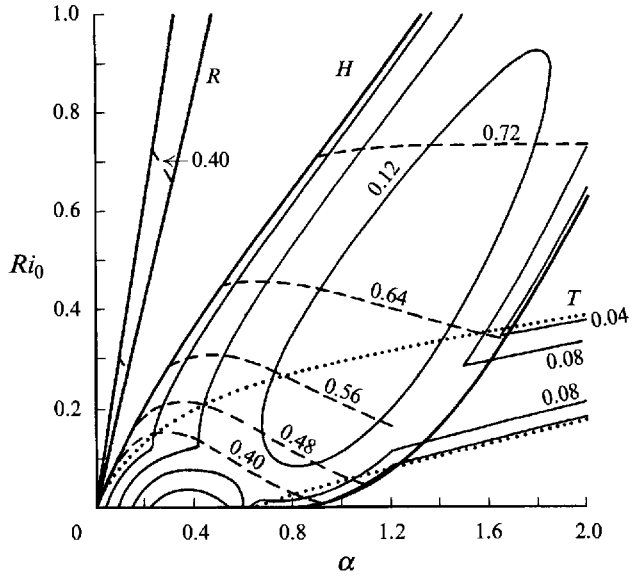

FIGURE 7. Stability boundary, with contours of growthrate (solid lines) of the most unstable mode at given wavenumber and Ri_0 and phase speed (dashed lines) for a three-layer flow with $R = 0.25$. Dotted lines denote the T mode boundaries. Contour intervals are as in figure 2.

where $\mathrm{d}/\mathrm{d}s$ is the derivative in the direction of increasing Ri_0, along the curve of maximal (with respect to wavenumber) σ_r, and σ_{rmax} is evaluated on this curve. From knowledge of the behaviour of the function

$$\sigma_{rmax}^2/Ri_0, \tag{4.26}$$

we may easily calculate the wavenumber and the angle at which it propagates of the most unstable three-dimensional mode for any actual background flow (with Richardson number Ri_1) provided (4.25) is satisfied for that flow. We simply calculate the maximum with respect to Ri_0 of (4.26), which we define to occur at Ri_2. From (4.26) we obtain the growthrate of the most unstable mode, and the wavenumber pertaining at that maximum is the magnitude of the wavenumber of the most unstable mode. Finally, the mode is uniquely determined to be propagating at an angle

$$\phi = \cos^{-1}\left(\frac{Ri_1}{Ri_2}\right)^{\frac{1}{2}}. \tag{4.27}$$

To illustrate the behaviour of the system, we choose the value $R = 0.25$ as a suitable generic case. Figure 7 is the stability boundary for $R = 0.25$, with contours of growthrate, and for the H and R mode branches, real phase speed. As is suggested by substitution of the asymptotic expressions for Ri_0 for an H mode (4.15) and an R mode (4.16), respectively, into the asymptotic form of the resonating positive phase speed internal wave of the instability (respectively c_{u+} in (4.6) and c_{l+} in (4.7)), the real phase speed of an R mode is typically smaller than that of an H mode for the same value of Ri_0. In both cases the phase speed of the mode increases as Ri_0 increases. As an aside, since R modes have smaller phase speeds than H modes for a given Ri_0, the region of overturning associated with the finite amplitude form of the R mode will be closer to the density interface than the region of overturning associated with an H mode. This suggests that R modes may lead to more mixing than an H mode with the same growthrate, even when the initial disturbance is purely two dimensional.

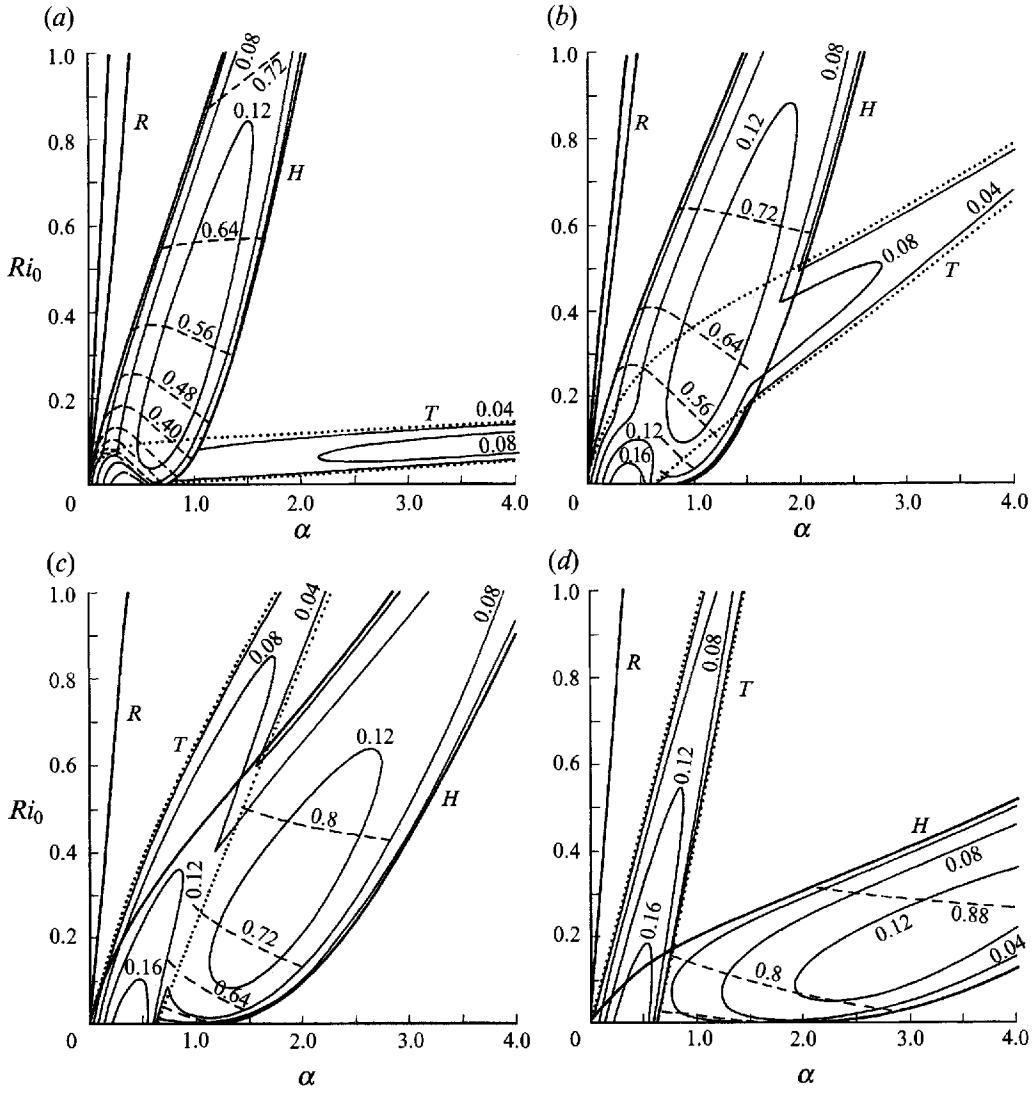

FIGURE 8. Stability boundaries, with contours of growthrate of the most unstable mode at given wavenumber and Ri_0 (solid lines) and phase speed (dashed lines) for three-layer flows with different values of R. Dotted lines denote the T mode boundaries. Contour intervals are as in figure 2. Note that phase speed contours are for the H mode and are only shown when the H mode is the mode with largest growthrate at that wavenumber and Ri_0: (*a*) $R = 0.1$; (*b*) $R = 0.3$; (*c*) $R = 0.5$; and (*d*) $R = 0.7$.

For this particular value of R, the growthrate of the T mode is initially the largest of the three branches for given Ri_0. However, the growthrate rapidly decays as Ri_0 increases, and then the H mode dominates, at least within the constraints of the linear theory. For both the R mode and the H mode the growthrate increases initially with Ri_0. The R mode attains its globally maximal growthrate at appreciably larger Ri_0 than the H mode.

The behaviour of the solutions as R is varied is quite complex, as is shown in figure 8. We consider the evolution of each branch separately. As R increases, the T mode appears at small Ri_0, and as R tends to 1, this branch approaches the result of Taylor.

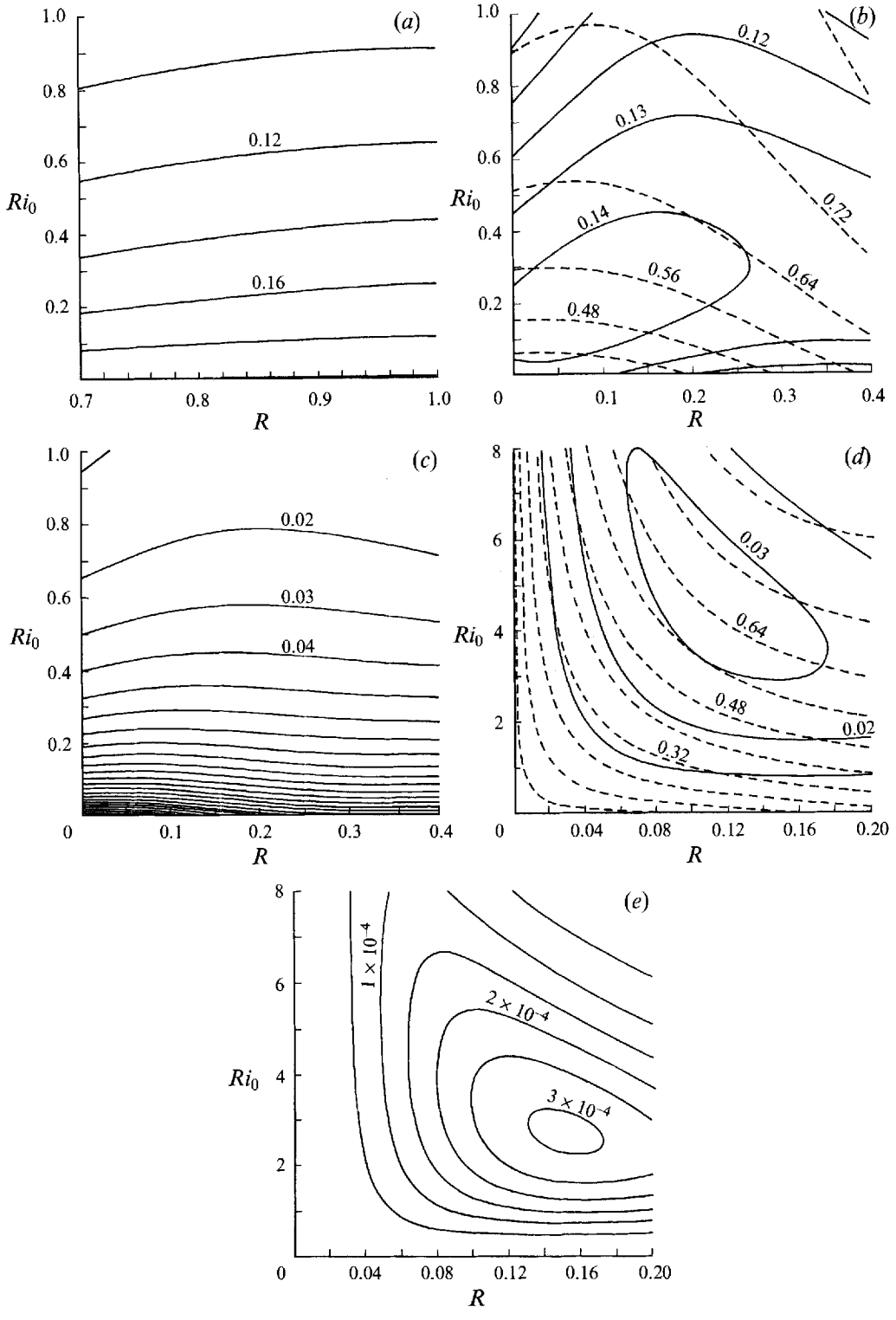

FIGURE 9. (*a*) Growthrate contours for the most unstable *T* mode, at given Ri_0, for various *R*. The contour interval is 0.02. (*b*) Growthrate (solid lines) and phase speed (dashed lines) for the most unstable *H* mode, at given Ri_0, for various *R*. The growthrate contour interval is 0.01, while the phase

In general the growthrate of the most unstable mode for a given Ri_0 decreases as Ri_0 is increased, but increases as R increases, as shown in figure 9(*a*). This behaviour definitely implies that T modes are primarily two-dimensionally unstable.

As R increases from 0 initially, the H mode branch moves to smaller α for given Ri_0 than the $R = 0$ situation considered by Holmboe. As R increases beyond about $1-1/\sqrt{2}$, however (as can be derived from comparison between (4.15) and the two layer result (2.19)), the H mode branch starts to move to large α, and eventually disappears at $R = 1$. For small Ri_0, we see the existence of H modes for $\alpha < \alpha_{crit}$ as defined by (4.17). As can be seen in figure 9(*b*), for sufficiently small R, the growthrate of the most unstable H mode initially increases with Ri_0, although never sufficiently rapidly to imply that the mode is subject to three-dimensional primary instabilities, even in the region where for infinitesimally small positive Ri_0, the flow is destabilized. (This is verified in figure 9(*c*), where we plot the expression (4.26) for the most unstable H mode. Note the monotonic decrease as Ri_0 increases.) The global maximum for growthrate of an H mode actually occurs at non-zero R (around $R = 0.08$ from figure 9*b*), and thus the presence of an intermediate layer actually may lead to the increased destabilization of the flow to Holmboe instability. At small Ri_0 and R, the growthrate of the L mode initially increases with Ri_0, but also never sufficiently swiftly to imply the existence of primary three-dimensional instability. Also, for certain intermediate Ri_0, the growthrate of a three-layer H mode is greater than that of the equivalent two-layer H mode for $R \leqslant \frac{1}{2}$.

Finally, the R mode branch emerges from the Ri_0 axis at small R, initially broadens and moves to larger α as R increases, and ultimately, as R tends to 1, narrows about its asymptotic result for $R = 1$ in (4.16). Considering the most unstable R mode, for given R the growthrate typically increases with Ri_0 quite rapidly, in general sufficiently quickly to imply three-dimensional primary instability (see figures 9(*d*) and 9(*e*), in particular the non-monotonic variation of (4.26)). For given Ri_0, the growthrate initially increases with R. However as R increases, the value Ri_{max} of Ri_0 at which, for given R the growthrate is globally maximized decreases as R decreases, and thus the region of primary three-dimensional instability of the mode considered in isolation decreases, as does the largest possible angle of cross-stream propagation.

However, for the R mode to dominate the flow, it is necessary for the R mode, for given Ri_0, to have larger growthrate than both the other two branches.

Thus, it is important to establish the region in (R, Ri_0) space where the R mode is both susceptible to a three-dimensional primary instability, and also has larger growthrate than both the H and T modes. This region is shown in figure 10(*a*). Three-dimensional primary instability is expected for some Ri_0 provided that $R \leqslant 0.095$. The maximum possible angle of propagation of a three-dimensional mode decreases as R increases, which can be verified by application of (4.27) for two separate values of R. For example, when $R = 0.01$, Ri_2, defined as above as the value of Ri_0 where (4.26) is maximized, is equal to 21.94. The smallest value of Ri_0 at which the R mode is globally the most unstable mode is $Ri_0 = 4.66$, thus predicting a maximal angle of propagation (from (4.27)) of about 62.6°. From figure 10(*a*), the corresponding values for a flow with $R = 0.02$ are $Ri_2 = 11.65$ and $Ri_1 = 4.14$ thus predicting a maximal angle of propagation of about 53.4°. As for the other characteristics of these three-

speed contour interval is 0.08. (*c*) σ_{rmax}^2/Ri_0 contours for the most unstable H mode, at given Ri_0, for various R. The contour interval is 0.01. (*d*) Growthrate (solid lines) and phase speed (dashed lines) for the most unstable R mode, at given Ri_0, for various R. The contour intervals are as in figure 9(*b*). (*e*) σ_{rmax}^2/Ri_0 contours for the most unstable R mode, at given Ri_0, for various R. The contour interval is 5.0×10^{-5}.

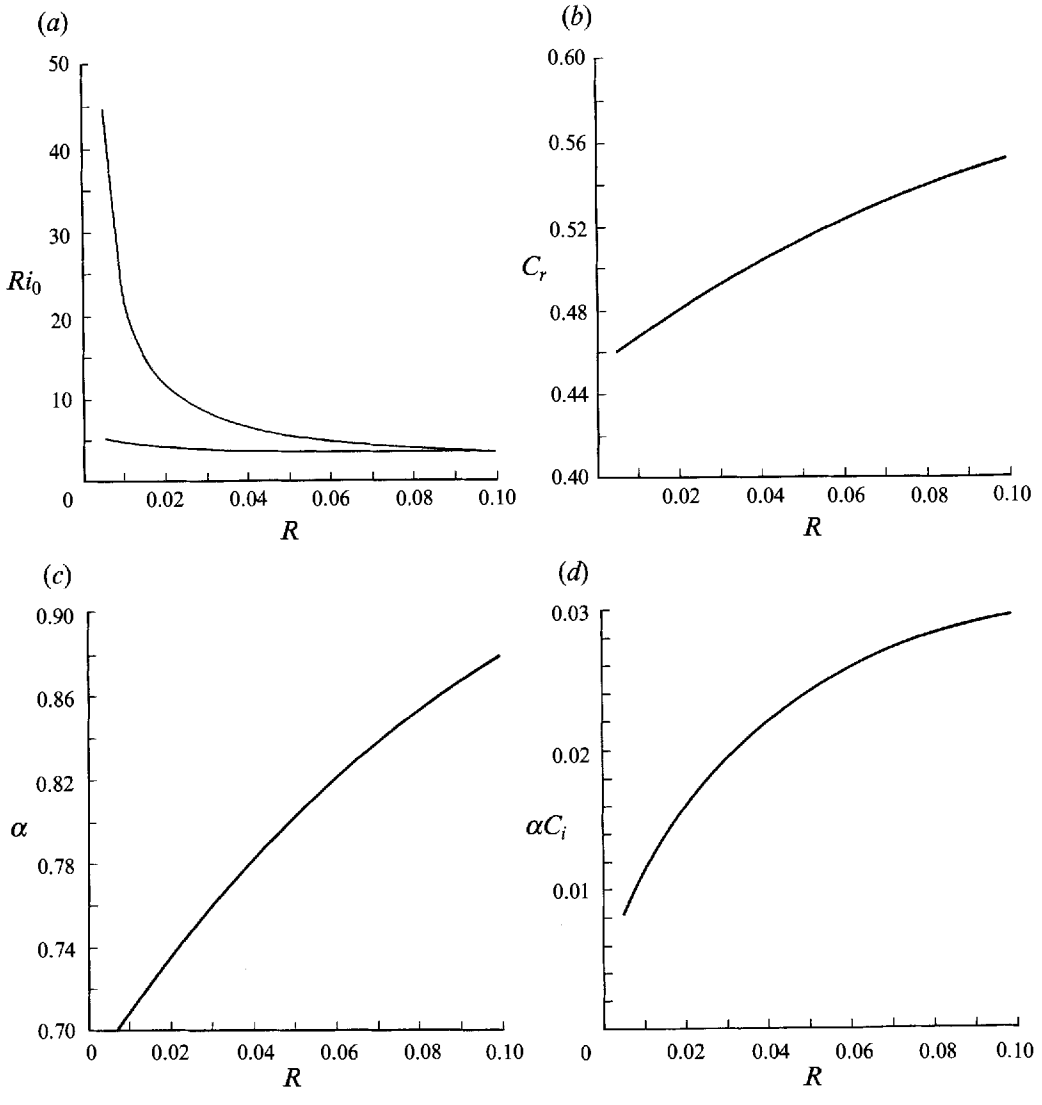

FIGURE 10. (*a*) Region of (R, Ri_0) space where the R mode is both the most unstable normal mode and susceptible to primary three-dimensional instabilities. (*b*) The phase speed of the globally most unstable R mode for various R. (*c*) The wavenumber of the globally most unstable R mode for various R. (*d*) The growthrate of the globally most unstable R mode for various R.

dimensional modes, the magnitudes of the phase speed, wavenumber and growthrate of this mode all increase monotonically with R as shown in figures 10(*b*)–10(*d*), respectively.

Thus, our calculations imply that flows where the density is layered are, for a wide range of Ri_0, initially unstable to multiple different disturbances, which may be considered as generalizations of the instabilities considered by Holmboe (1962) as well as purely unstable zero phase speed disturbances analogous to those considered by Taylor (1931). If there is a thin central density layer, such shear flows are predicted to be most unstable to disturbances propagating at an angle to the mean flow, and thus the flow must, from the outset, be considered in its full three dimensions. When the R mode is susceptible to primary three-dimensional instability, the flow will attempt to

generate vorticity with some spanwise component. Thus the perturbation of the density interfaces is likely to be highly complex, and may lead to significantly enhanced mixing.

4.5 *Resonant triads*

For intermediate R, the H mode is still the most unstable mode for intermediate Ri_0, and as mentioned above, the growthrate is often larger than that suggested by the two-layer calculations. Only for very large R does linear stability theory predict that the most unstable mode for given Ri_0 is likely to be of T mode type. Thus, linear theory predicts that unless the density and shear layer lengthscales are closely matched, the flow will primarily be susceptible to H mode type disturbances, and they should dominate at intermediate values of Ri_0.

However, because of the multiple possible modes supported by the flow that we are considering, the possibility for resonance between three waves within the system cannot be discounted. In particular, for any given Ri_0, there are typically five waves that are predicted to undergo, at least initially, exponential growth. If three of these waves could resonate when they reached finite amplitude, their amplification, and hence the approach to breakdown and mixing of the background flow, might be significantly enhanced.

It is well known (see Craik 1985) that three modes, with real phase speeds c_1, c_2 and c_3, and wavenumbers α_1, α_2 and α_3 form a so-called resonant triad, and hence wave 1 and wave 2 may possibly resonate to amplify wave 3, if

$$\alpha_3 = \alpha_1 + \alpha_2, \tag{4.28}$$

$$\alpha_3 c_3 = \alpha_1 c_1 + \alpha_2 c_2. \tag{4.29}$$

Of particular interest is resonance between modes that are already linearly unstable, as such modes have a well-understood route to finite amplitude and may then be preferentially amplified to dominance of the flow, even if their linear growthrates are quite small. Since the H mode branch actually consists of two unstable modes each at the same wavenumber α_H with equal and opposite real phase speed, and the T mode branch consists of zero real phase speed instabilities with wavenumber α_T, a resonant triad between a T mode and the two constituent parts of an H mode requires that

$$\alpha_T = 2\alpha_H, \tag{4.30}$$

as (4.29) is automatically satisfied, since $c_T = 0$ and $\alpha_1 = \alpha_2 = \alpha_H, c_1 = -c_2 = c_H$ by the symmetry of the system.

From figures 8(*a*) and 8(*b*), the T mode branch, is, for smaller R, typically at larger α than the H mode branch. Indeed, from comparison of the asymptotic results for the T mode branch (4.12) and the H mode branch (4.15), the resonance condition (4.30) implies that, at large α,

$$\frac{Ri_0}{(1-R)^2} + \frac{2}{(1-R)} = \frac{Ri_0}{2R^2}, \tag{4.31}$$

or

$$-4R^3 + R^2(4+Ri_0) + 2Ri_0 R - Ri_0 = 0, \tag{4.32}$$

which in the limit of large Ri_0 implies that

$$R = \sqrt{2} - 1. \tag{4.33}$$

Thus, for $R < 0.4$, there is at least the possibility that nonlinear resonance may take place for some Ri_0 between the H modes and the T mode, though no attempt has been made to calculate the interaction coefficients.

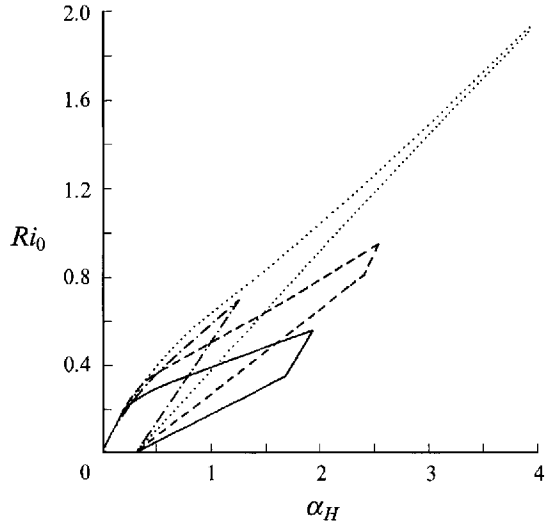

FIGURE 11. Region of $\alpha_H - Ri_0$ space where it is possible for the T mode to form a resonant triad with the H mode waves for $R = 0.25$ (solid lines), $R = 0.3$ (dashed lines), $R = 0.35$ (dotted lines) and $R = 0.4$ (dot–dashed lines).

In figure 11, we show the regions of (α_H, Ri_0) parameter space where (4.30) is satisfied for several values of R. There is the possibility of nonlinear resonance for a wide variety of initial background flows. For small R, the region of (α_H, Ri_0) space where nonlinear resonance may be possible is restricted to small Ri_0. However, as R increases, and thus, as can be seen in figure 8, the T mode branch moves to smaller α for given Ri_0, the region for possible resonance increases in area, and the maximal Ri_0 for the possibility of resonance increases in value. Ultimately, however, the H mode branch starts to move to larger α, and around $R = 0.373$, the two mode branches pass through a critical condition, namely

$$\alpha_{SH} = 2\alpha_{LT}, \tag{4.34}$$

for some Ri_0, where α_{SH} is the locus of wavenumbers defining the smaller α stability boundary for the H mode, while α_{LT} is the locus of wavenumbers defining the larger α stability boundary for the T mode. For values of R larger than that which first satisfies (4.34) the region of possible nonlinear resonance rapidly shrinks, and as R increases, the formation of a nonlinear triad is once again only possible for very small Ri_0. For intermediate values of R the flow may be able to excite resonant triads of linearly unstable modes for flows with significant Ri_0.

It is important to stress that nonlinear resonance within this flow does not require the consideration of modes propagating at an angle to the mean flow (see Craik 1968) owing to the properties of the eigenvalue equation (3.33). The calculation of the actual coefficients of interaction has not been conducted. Nevertheless, it is possible that, for flows at small R, although the linear growthrate of the T mode is appreciably smaller than that of the H modes at intermediate Ri_0, the T modes may be preferentially amplified by a resonance with these H modes, and hence grow to finite amplitude. Thus, even for relatively narrow intermediate layers, significant overturnings in the interior of the layer are not to be totally discounted, although a conventional interpretation would be that in a laboratory or geophysical flow the most unstable H modes would be the dominant structures at finite amplitude. We have demonstrated

that, far from being restricted to the $R = 1$ case initially considered by Taylor, T mode type instabilities are to be expected in multi-layer stratified shear flows, even when the intermediate layer is relatively narrow, and they are likely to be associated with H modes, growing within the same flow.

5. Conclusions

The existence of an intermediate region of intermediate density, within a shear layer of piecewise constant vorticity leads to the development of generalizations of the previously observed forms of instability discussed by Holmboe and Taylor, which we refer to as H modes and T modes, whose properties are altered by the intermediate density region in a non-trivial way. The ratio R (defined by (3.1)) of the depths of the intermediate density layer and the shear layer is a very important parameter to describe the qualitative behaviour of the linear stability of the flow.

The two modes in general will appear within the same flow for all Ri_0, and the two previously studied cases discussed in §2 are seen to be highly critical limiting cases of a more general class of flows. The presence of an intermediate density region implies that Holmboe waves can have larger growthrates than those predicted by two-layer models over a very large range of intermediate layer widths up to $R = \frac{1}{2}$. Also, for $R < 0.4$, there is a wide range of Ri_0 over which there is the possibility of nonlinear resonance between the two different modes. Thus, even where the linear growthrate of the T mode is quite small relative to that of the H mode (i.e. flows where R is appreciably less than 1), the possibility of T modes appearing at finite amplitude cannot be discounted.

Since we are likely to have an intermediate region in any physically realizable flow, we thus expect the phenomenon of both Holmboe wave type and T mode type solutions to be more common than previously assumed, since we see that their existence is predicted for all $R < 1$.

We map the transition from H to T mode type solutions with R and see that the stratified T mode type solution has a very different growth mechanism from that of the instability first considered by Rayleigh in a homogeneous shear layer.

For both these modes we see that a vital destabilizing mechanism is the statically stable density distribution. H modes can be thought of as being destabilized by an interaction between an internal wave on a density interface and a Rayleigh wave on the nearer vorticity interface, while T modes are implicitly driven by an interaction between internal waves on the two density interfaces. Thus it is an over-simplification to believe that H modes are only of importance when the intermediate layer is arbitrarily narrow in width.

For certain parameter ranges we also observe the existence of a new form of instability, which we refer to as the R mode. This instability is triggered by an interaction between waves on a density interface and the further vorticity interface. It is oscillatory, with a smaller phase speed than that of the H mode.

Modes within the new region of instability can be both globally the most unstable mode, and also primarily unstable to a disturbance propagating at a non-zero angle to the mean flow, since the growthrate of the most unstable mode within this region increases sufficiently quickly with Ri_0 in certain circumstances, in particular when the two density interfaces are close together. Since modes propagating at an angle 'feel' a larger Ri_0, they have the potential to have larger growthrate.

This behaviour is predicted to occur for narrow intermediate density regions and large Ri_0. Such situations arise naturally during laboratory experiments. (Narimousa

& Fernando 1987) on notionally two-layer flows. Thus the presence of this new, theoretically dominant mode of instability for a stratified shear layer may be significant in assessing the mixing in shear flows at high Ri_0.

Since the function (4.23) whose behaviour predicts the existence of a three-dimensional primary instability is an even function of this angle of propagation to the mean flow, when we have three-dimensional behaviour we expect to see two modes, which should constructively interfere with each other, and thus lead to a highly non-uniform cross-stream structure. From laboratory evidence (see Lawrence *et al.* 1991), the onset of significant cross-stream inhomogeneities may be closely followed by a breakdown in the flow organization and the onset of mixing. Such mixing is significantly more intense than that associated with the finite amplitude form of, at least approximately, two-dimensional Holmboe modes (see Browand & Winant 1973).

Previous work (Smyth & Peltier 1990) has only predicted the existence of three-dimensional primary instability for flows with $200 \leqslant Re \leqslant 400$, which is several orders of magnitude smaller than typical Reynolds numbers in the atmosphere or the ocean. The transition to three-dimensional behaviour (and hence to enhanced mixing, an increase in R, and ultimately the dominance of billows) through a secondary instability of the finite amplitude forms of the modes is likely to be important and relevant, (see Thorpe 1987) especially since it is well known that in a homogeneous flow billow type structures are subject to a cross-stream instability owing to streamwise vorticity. Analysis of the stratified analogue of such behaviour is clearly beyond the scope of this linear theory. However, the demonstration that it is possible for an inviscid flow to be subject to a primary three-dimensional instability shows that we must be extremely careful in our application of the commonly used two-dimensional models, whether linear or nonlinear, to realistic situations with a thin intermediate density region.

This paper discusses some of the results in the author's PhD thesis. Thanks are due to Dr P. F. Linden for many useful discussions. The support of a College studentship from Churchill College, Cambridge is gratefully acknowledged, as is an SERC CASE award with the Health and Safety Executive, Sheffield. Preparation of the manuscript was supported by the Japan Canada Project in Weather and Climate of the Arctic at the University of Toronto.

Appendix A. Calculation of discriminant D

The discriminant D, defined by (4.13), may be expressed as a sixth-order polynomial in Ri_0:

$$b_0 Ri_0^6 + b_1 Ri_0^5 + b_2 Ri_0^4 + b_3 Ri_0^3 + b_4 Ri_0^2 + b_5 Ri_0 + b_6 = 0. \tag{A 1}$$

The b_i are defined as follows:

$$b_0 = \frac{-x_1^2 y_2^2}{108} + \frac{y_2^3}{27}, \tag{A 2}$$

$$b_1 = \frac{-x_1^2 y_1 y_2}{54} - \frac{x_0 x_1 y_2^2}{54} + \frac{y_1 y_2^2}{9} + \frac{x_1^3 z_2}{27} - \frac{x_1 y_2 z_2}{6}, \tag{A 3}$$

$$b_2 = \frac{-x_1^2 y_1^2}{108} - \frac{x_1^2 y_0 y_2}{54} - \frac{x_0 x_1 y_1 y_2}{27} + \frac{y_1^2 y_2}{9} - \frac{x_0^2 y_2^2}{108} + \frac{y_0 y_2^2}{9} + \frac{x_1^3 z_1}{27} - \frac{x_1 y_2 z_1}{6}$$
$$+ \frac{x_0 x_1^2 z_2}{9} - \frac{x_1 y_1 z_2}{6} - \frac{x_0 y_2 z_2}{6} + \frac{z_2^2}{4}, \tag{A 4}$$

$$b_3 = \frac{-x_1^2 y_0 y_1}{54} - \frac{x_0 x_1 y_1^2}{54} + \frac{y_1^3}{27} - \frac{x_0 x_1 y_0 y_2}{27} - \frac{x_0^2 y_1 y_2}{54} + \frac{2 y_0 y_1 y_2}{9} + \frac{x_1^3 z_0}{27} - \frac{x_1 y_2 z_0}{6}$$
$$+ \frac{x_0 x_1^2 z_1}{9} - \frac{x_1 y_1 z_1}{6} - \frac{x_0 y_2 z_1}{6} + \frac{x_0^2 x_1 z_2}{9} - \frac{x_1 y_0 z_2}{6} - \frac{x_0 y_1 z_2}{6} + \frac{z_1 z_2}{2}, \quad \text{(A 5)}$$

$$b_4 = \frac{-x_1^2 y_0^2}{108} - \frac{x_0 x_1 y_0 y_1}{27} - \frac{x_0^2 y_1^2}{108} + \frac{y_0 y_1^2}{9} - \frac{x_0^2 y_0 y_2}{54} + \frac{y_0^2 y_2}{9} + \frac{x_0 x_1^2 z_0}{9} - \frac{x_1 y_1 z_0}{6} - \frac{x_0 y_2 z_0}{6}$$
$$+ \frac{x_0^2 x_1 z_1}{9} - \frac{x_1 y_0 z_1}{6} - \frac{x_0 y_1 z_1}{6} + \frac{z_1^2}{4} + \frac{x_0^3 z_2}{27} - \frac{x_0 y_0 z_2}{6} + \frac{z_0 z_2}{2}, \quad \text{(A 6)}$$

$$b_5 = \frac{-x_0 x_1 y_0^2}{54} - \frac{x_0^2 y_0 y_1}{54} + \frac{y_0^2 y_1}{9} + \frac{x_0^2 x_1 z_0}{9} - \frac{x_1 y_0 z_0}{6} - \frac{x_0 y_1 z_0}{6} + \frac{x_0^3 z_1}{27} - \frac{x_0 y_0 z_1}{6} + \frac{z_0 z_1}{2}, \quad \text{(A 7)}$$

$$b_6 = \frac{-x_0^2 y_0^2}{108} + \frac{y_0^3}{27} + \frac{x_0^3 z_0}{27} - \frac{x_0 y_0 z_0}{6} + \frac{z_0^2}{4}, \quad \text{(A 8)}$$

where

$$x_0 = -2R^2 + \frac{e^{-4\alpha} - (2\alpha - 1)^2}{4\alpha^2}, \quad \text{(A 9)}$$

$$x_1 = -1/\alpha, \quad \text{(A 10)}$$

$$y_0 = -2R^2 \left(\frac{e^{-4\alpha} - (2\alpha - 1)^2}{4\alpha^2} \right) + R^4, \quad \text{(A 11)}$$

$$y_1 = \left(\frac{e^{-4\alpha} + (2\alpha - 1)^2}{4\alpha^3} \right) - R^2/\alpha + \frac{e^{-2\alpha}}{\alpha^2} \left(2R \sinh 2\alpha R + \frac{(2\alpha - 1)}{2\alpha} \cosh 2\alpha R \right), \quad \text{(A 12)}$$

$$y_2 = \frac{1 - e^{-4\alpha R}}{4\alpha^2}, \quad \text{(A 13)}$$

$$z_0 = R^4 \left(\frac{e^{-4\alpha} - (2\alpha - 1)^2}{4\alpha^2} \right), \quad \text{(A 14)}$$

$$z_1 = R^2 \left(\frac{e^{-4\alpha} + (2\alpha - 1)^2}{4\alpha^3} \right) + \frac{R^2 e^{-2\alpha} (2\alpha - 1) \cosh 2\alpha R}{2\alpha^3}, \quad \text{(A 15)}$$

$$z_2 = \frac{e^{-4\alpha}(1 - e^{4\alpha R}) - (2\alpha - 1)^2 (1 - e^{-4\alpha R})}{16\alpha^4} - \frac{e^{-2\alpha} (2\alpha - 1) \sinh 2\alpha R}{4\alpha^4}. \quad \text{(A 16)}$$

The x_n, y_n and z_n are simply the coefficients of Ri_0^n in a_2, a_4 and a_6, respectively, defined by (3.34)–(3.36). From (A 9), (A 11) and (A 14), (A 8) implies that $b_6 = 0$ as stated in §4.2.

Appendix B. H modes at small Ri_0

For small $|Ri_0|$, the sign of D, and hence the stability of the normal modes of the system, is determined by the sign of b_5 in (4.14). We are interested in the behaviour of D for wavenumbers close to α_{crit} defined by (4.17). For a given value of R, let us consider disturbances with wavenumber α_p where α_p is defined by

$$R^2 = \frac{(2\alpha_p - 1)^2 - e^{-4\alpha_p}}{4\alpha_p^2} - \epsilon, \quad \text{(B 1)}$$

for some small parameter

$$\epsilon \ll \frac{(2\alpha_p - 1)^2 - e^{-4\alpha_p}}{4\alpha_p^2}. \tag{B 2}$$

We note that when $\epsilon > (<) 0$, $\alpha_p > (<) \alpha_{crit}$. We may substitute for R^2 through use of (B 1) into the expression for b_5, i.e. (A 7), using binomial expansions where necessary. The expression for b_5 becomes

$$b_5 = \frac{-\exp(-2\alpha_p) X \epsilon^3}{9\alpha_p^3} (\tfrac{1}{3}\exp(-2\alpha_p) + \tfrac{1}{4}(2\alpha_p - 1)\cosh 2\alpha_p X^{\frac{1}{2}} + \tfrac{2}{3}\alpha_p X^{\frac{1}{2}} \sinh 2\alpha_p X^{\frac{1}{2}}) + o(\epsilon^4), \tag{B 3}$$

where

$$X \equiv \frac{(2\alpha_p - 1)^2 - e^{-4\alpha_p}}{4\alpha_p^2}. \tag{B 4}$$

From (B 3), since $\alpha_p > 0.64$ for all non-zero R, and hence $X > 0$, b_5 is opposite in sign to ϵ, for small ϵ. Thus b_5 is opposite in sign to $\alpha_p - \alpha_{crit}$, and hence when $\alpha_p - \alpha_{crit} < 0$, then $b_5 > 0$, and so $D > 0$ for small enough positive Ri_0. This implies that the eigenvalue equation (3.33) has complex conjugate solutions for $Ri_0 > 0$, and real solutions for $Ri_0 < 0$, as required.

REFERENCES

BATCHELOR, G. K. 1967 *An Introduction to Fluid Dynamics*. Cambridge University Press.

BROWAND, F. K. & WINANT, C. D. 1973 Laboratory observations of shear layer instability in a stratified fluid. *Boundary-Layer Met.* **5**, 67–87.

CAIRNS, R. A. 1979 The role of negative energy waves in some instabilities of parallel flows. *J. Fluid Mech.* **92**, 1–14.

CRAIK, A. D. D. 1968 Resonant gravity-wave interactions in a shear flow. *J. Fluid Mech.* **34**, 531–549.

CRAIK, A. D. D. 1985 *Wave interactions and fluid flows*. Cambridge University Press.

GILL, A. E. 1982 *Atmosphere Ocean Dynamics*. Academic.

HAYASHI, Y.-Y. & YOUNG, W. R. 1987 Stable and unstable shear modes of rotating parallel flows in shallow water. *J. Fluid Mech.* **184**, 477–504.

HAZEL, P. 1972 Numerical studies of the stability of inviscid stratified shear flows. *J. Fluid Mech.* **51**, 39–61.

HOILAND, E. 1948 Stability and instability waves in sliding layers with internal stability. *Arch. Math. og Nat.* **L**, no. 3.

HOLMBOE, J. 1962 On the behaviour of symmetric waves in stratified shear layers. *Geofys. Publ.* **24**, 67–113.

HOWARD, L. N. & MASLOWE, S. A. 1973 Stability of stratified shear flow. *Boundary-Layer Met.* **4**, 511–523.

LAWRENCE, G. A., BROWAND, F. K. & REDEKOPP, L. G. 1991 The stability of a sheared density interface. *Phys. Fluids* A **3**, 2360–2370.

LINDEN P. F. 1979 Mixing in stratified fluids. *Geophys. Astrophys. Fluid Dyn.* **13**, 1–23.

NARIMOUSA, S. & FERNANDO, H. J. S. 1987 On the sheared density interface of an entraining stratified fluid. *J. Fluid Mech.* **174**, 1–22.

RAYLEIGH, LORD 1894 *The Theory of Sound*, 2nd edn. Macmillan.

REDONDO, J. M. R. 1989 Internal and external mixing in stratified-shear flow. In *Advances in Turbulence 2* (ed. H.-H. Fernholz & H. E. Fiedler). Springer.

SMYTH, W. D. & PELTIER, W. R. 1990 Three-dimensional primary instability of a stratified dissipative parallel flow. *Geophys. Astrophys. Fluid Dyn.* **52**, 249–261.

SMYTH, W. D., KLAASEN, G. P. & PELTIER, W. R. 1988 Finite amplitude Holmboe waves. *Geophys. Astrophys. Fluid Dyn.* **43**, 181–222.

SQUIRE, H. B. 1933 On the stability of three-dimensional disturbances of viscous flow between parallel walls. *Proc. R. Soc. Lond.* A **142**, 621–628.

STEPHENSON, P. W. & FERNANDO, H. J. S. 1991 Turbulence and mixing in a stratified shear flow. *Geophys. Astrophys. Fluid Dyn.* **59**, 147–164.

TAYLOR, G. I. 1931 Effect of variation in density on the stability of superposed streams of fluid. *Proc. R. Soc. Lond.* A **132**, 499–523.

THORPE, S. A. 1973 Turbulence in stably stratified fluids: a review of laboratory experiments. *Boundary-Layer Met.* **5**, 95–119.

THORPE, S. A. 1987 Transitional phenomena and the development of turbulence in stratified fluids: a review. *J. Geophys. Res.* **92**, C, 5231–5248.

TURNER, J. S. 1973 *Buoyancy Effects in Fluids.* Cambridge University Press.

YIH, C.-S. 1955 Stability of two-dimensional parallel flows for three-dimensional disturbances. *Q. Appl. Maths* **12**, 434–435.